中国科学: 地球科学 2020 年 第 50 卷 第 12 期: 1845 ~ 1873
SCIENTIA SINICA Terrae earthcn.scichina.com
《中国科学》杂志社 SCIENCE CHINA PRESS

综 述

汇聚板块边缘的埃达克质岩: 成分和成因

王强[1,2,3*], 郝露露[1], 张修政[1], 周金胜[1], 王军[1], 李奇维[1], 马林[1], 张龙[1], 齐玥[1], 唐功建[1], 但卫[1], 范晶晶[1]

1. 中国科学院广州地球化学研究所同位素地球化学国家重点实验室, 广州 510640;
2. 中国科学院大学地球与行星科学学院, 北京 100049;
3. 中国科学院青藏高原地球科学卓越创新中心, 北京 100101
* 通讯作者, E-mail: wqiang@gig.ac.cn

收稿日期: 2020-02-20; 收修改稿日期: 2020-09-05; 接受日期: 2020-09-08; 网络版发表日期: 2020-11-05
国家自然科学基金重点项目(批准号: 41630208和91855215)、第二次青藏高原综合科学考察研究专题项目(编号: 2019QZKK0700)、国家重点研发计划项目(编号: 2016YFC0600407)、中国科学院战略性先导科技专项A类项目(编号: XDA2007030402)和广州市重点项目(编号: 201707020032)资助

摘要 埃达克质岩是一类中酸性岩浆岩, 在地球化学上以富集轻稀土元素、亏损重稀土元素、具有正的或者无Eu-Sr异常以及高的La/Yb和Sr/Y比值为特征. 新生代火山弧环境中由俯冲洋壳(板片)在榴辉岩相条件下部分熔融形成的埃达克质岩属于狭义的埃达克岩, 主要出现于环太平洋火山弧区(洋内弧、大陆弧、陆缘岛弧). 而新生代由碰撞加厚下地壳部分熔融形成的埃达克质岩主要出现在特提斯-青藏高原碰撞带. 在火山弧区, 俯冲板片熔融产生的埃达克质岩浆可以交代地幔楔形成一套特殊的岩石组合——埃达克岩-埃达克型高镁安山岩-Piip型高镁安山岩-富Nb玄武岩-玻安山岩等, 不同于俯冲大洋板片流体交代地幔楔形成的玄武岩-安山岩-英安岩-流纹岩组合. 大量资料显示, 基性岩熔融产生埃达克质熔体的条件为压力1.2~3.0GPa、温度800~1000℃、H_2O含量1.5~6.0wt.%, 源区残留矿物组合为石榴石+金红石, 很少或无斜长石. 新生代铜金等矿床的分布与新生代埃达克质岩的分布区一致, 并且一些矿床的成矿母岩就是埃达克质岩. 因此, 埃达克质岩不仅具有重要的地球深部动力学指示意义, 也具有重要的铜金成矿指示意义及勘探价值. 尽管对新生代埃达克质岩的研究取得了一些进展, 但仍然在一些领域存在薄弱点, 包括前新生代埃达克质岩的构造背景、成因、岩浆起源、熔体-地幔作用及其与板块构造启动、地壳生长的关联等. 未来需要研究的领域包括: 不同类型岩石(包括中酸性岩浆岩)在不同温压条件下熔融和分离结晶过程的实验模拟与埃达克质岩浆的产生、岩浆储库演化与埃达克质岩的形成、前新生代埃达克质岩构造背景与成因及动力学过程、板片熔体与地幔相互作用及交代作用、太古宙埃达克质英云闪长岩岩-奥长花岗岩-花岗闪长岩(TTG)的形成与板块构造启动及地壳生长、不同构造背景中埃达克质岩的形成与金属成矿等.

关键词 埃达克岩, 俯冲带, 碰撞带, 成因, 成矿, 动力学

中文引用格式: 王强, 郝露露, 张修政, 周金胜, 王军, 李奇维, 马林, 张龙, 齐玥, 唐功建, 但卫, 范晶晶. 2020. 汇聚板块边缘的埃达克质岩: 成分和成因. 中国科学: 地球科学, 50(12): 1845–1873, doi: 10.1360/SSTe-2020-0034
英文引用格式: Wang Q, Hao L, Zhang X, Zhou J, Wang J, Li Q, Ma L, Zhang L, Qi Y, Tang G, Dan W, Fan J. 2020. Adakitic rocks at convergent plate boundaries: Compositions and petrogenesis. Science China Earth Sciences, 63(12): 1992–2016, https://doi.org/10.1007/s11430-020-9678-y

1 引言

自从20世纪60~70年代板块构造理论创立以来, 弧岩浆岩的成因受到了广泛关注(Frisch等, 2011). 其中, 玄武岩-安山岩-英安岩-流纹岩组合的起源成为与弧系统演化相关的最重要的岩石学问题(Ringwood, 1974). 弧玄武岩来自地幔楔的熔融, 但形成于弧环境中的中酸性岩(如安山岩、英安岩和流纹岩)的成因则存在激烈的争议. 作为一种稀有的弧岩浆岩, 埃达克岩最早是由Defant和Drummond(1990)提出来的, 其原始的定义是指在现代弧环境中, 由俯冲的年轻(≤25Ma)玄武质洋壳在榴辉岩相的条件下熔融形成的强烈亏损重稀土元素(HREE)(如Yb≤1.90ppm, 1ppm=1μg g^{-1})与Y(≤18ppm)、富Sr(一般≥400ppm)、高La/Yb(≥20)与Sr/Y(≥40)比值的中酸性(SiO_2≥56.0wt.%)钙碱性火山岩(安山岩、英安岩和流纹岩)及相应的侵入岩(英云闪长岩、奥长花岗岩). 由于这种由俯冲洋壳熔融形成的新生代弧岩浆岩最先在美国阿留申群岛中Adak(埃达克)岛被发现(Kay, 1978), 因此, Defant和Drummond(1990)将其命名为埃达克岩. 埃达克岩的概念提出来以后, 由于该类岩石具有重要的地球动力学、金属成矿意义, 受到了广泛关注, 成为固体地球科学研究的重要热点之一.

随着研究的深入, 科学家们发现除了新生代火山弧区(如环太平洋)外, 具有同样地球化学特征的岩石不仅出现在新生代碰撞带(如特提斯-青藏高原)中(例如, Chung等, 2003; Hou等, 2004)和高原内部(如可可西里、羌塘)(例如, Wang等, 2005, 2008), 而且在一些前新生代(包括中生代、古生代、元古代和太古宙等)火成岩中, 也出现大量与埃达克岩具有类似地球化学特征的岩石(例如, Martin, 1999; 张旗等, 2001; Xu等, 2002; Gao等, 2004; Martin等, 2005; Wang等, 2006a, 2006b). 这些岩石的形成除了与俯冲洋壳熔融有关之外, 也可能与大陆俯冲、碰撞、地壳增厚与拆沉、岩浆底侵或混合、熔体-地幔作用等深部动力学过程密切相关, 部分岩石伴随铜金成矿作用(例如, 张旗等, 2001; Defant等, 2002; 王强等, 2001a, 2003, 2007, 2008).

尽管该类岩石成因具有重要研究意义, 但如何更好地给该类岩石命名受到关注(例如, Tarney和Jones, 1994; Harris等, 1996; Yumul等, 2000; Conrey等, 2001; Sheppard等, 2001; 张旗等, 2001; 葛小月等, 2002; Zeng等, 2011). 特别是, 一些岩石除了重要地球化学特征与埃达克岩类似外, 并不出现于火山弧环境, 也并不是由俯冲洋壳熔融形成, 这与原始定义中"埃达克岩"的成因存在差别. 针对这个问题, 我们认为需要把握一个基本原则: 作为一个岩石名称不应该以岩石的成因、构造背景为前提, 而应该反映该岩石最基本的特征, 这个特征不会随人们对岩石成因、构造背景的认识不同而改变(王强等, 2008; Wang等, 2007a). 基于上述原则, 尽管这些岩石的成因和形成的动力学背景存在差异, 元素和同位素组成也不尽相同, 但它们都具有一个共同的岩石地球化学特征, 即普遍含有长石、角闪石和黑云母等矿物, 岩石类型主要为安山质、英安质和流纹质岩石和相应的侵入岩, 为中酸性(SiO_2≥56.0 wt.%), 富集轻稀土元素(LREE)但强烈亏损重稀土元素(如, Yb≤1.9ppm)和Y元素(≤18ppm), 富Sr(一般≥400ppm)、高La/Yb(≥20)与Sr/Y(≥40)比值, 无或正Sr-Eu异常(例如, Le Maitre, 2002; Castillo, 2006, 2012; 王强等, 2008). 因此, 本文把具有上述共同特征的岩石统称为"埃达克质岩"(王强等, 2008; Wang等, 2007a). 按照这个标准, Defant和Drummond(1990)提出的弧环境中由俯冲洋壳熔融形成的埃达克岩也可以归入"埃达克质岩"的范畴.

地质学一个最基本的原理是"将今论古". 因此, 研究年轻的(即新生代)的、构造背景清楚的埃达克质岩及成矿作用, 将会为深入探究前新生代这类岩石的成因及其动力学、成矿意义提供重要启示. 由于新生代埃达克质岩主要出现在汇聚板块边缘, 因此, 本文在回顾俯冲洋壳熔融与埃达克质岩研究历史相关内容的基础上, 重点介绍新生代埃达克质岩及其产生的岩石组合的研究进展, 同时综述埃达克质岩浆产生的条件及成矿意义, 并讨论埃达克质岩研究存在的问题和展望未来需要研究的领域.

2 俯冲洋壳熔融与埃达克岩概念的提出

自从20世纪60年代末期板块构造理论诞生以来, 有关俯冲大洋地壳能否在榴辉岩相条件下发生熔融形成弧岩浆岩, 一直存在争议.

一部分学者认为, 俯冲洋壳在榴辉岩相条件下的熔融在中酸性岩浆岩的成因中发挥了作用. 在1968年,

基于熔融实验研究，Green和Ringwood(1968)提出了钙碱性中酸性火成岩有可能由进入到地幔100~150km深处的榴辉岩(原岩为洋中脊玄武岩(MORB))熔融形成, 源区残留物为辉石+斜长石+少量石榴石. 针对太古宙大陆地壳的生长与演化问题，Arth和Hanson(1972, 1975)最早提出晚太古宙(2.7Ga)英云闪长岩-奥长花岗岩-花岗闪长岩(TTG)强烈亏损HREE(如Yb=0.02~1.20ppm)，是由于这些岩石可能是玄武质岩石在俯冲过程中或在堆积增厚的条件下熔融形成的，熔融残留物是石榴石+辉石. Nicholls(1974)和Ringwood(1974)则提出了弧钙碱性中酸性岩浆岩的三阶段演化模式: (1) 石英榴辉岩(俯冲板片)部分熔融产生流纹质-英安质熔体; (2) 这类长英质熔体与上覆橄榄岩发生反应形成辉石岩; (3) 辉石岩发生熔融形成镁铁质岩浆, 该岩浆进一步演化(如分离结晶)，然后产生了这些钙碱性岩浆岩. 一些科学家曾将上述模式应用于解释环太平洋新生代火山弧中一些中酸性岩浆岩的形成. 例如, 基于对智利一些新生代稀土元素强烈分异(La/Yb≥15)并强烈亏损HREE(Yb=0.70~1.9ppm)的中酸性火山岩和花岗岩类的研究，Thorpe等(1976)以及López-Escobar等(1977, 1979)认为这些岩石的形成可能类似于上述三阶段演化模式. Kay(1978)通过对美国阿留申群岛中埃达克岛上新生代一种富含普通辉石斑晶(缺少橄榄石)以及斜长石、普通辉石微晶的高镁安山岩的研究，发现该岩石强烈亏损HREE(Yb<1.00ppm，La/Yb≥40)且高MgO(≥4.50wt.%)，提出其是由俯冲的玄武质洋壳在榴辉岩相条件下熔融形成的岩浆与地幔楔橄榄岩发生交换反应后形成的. 进入20世纪80年代, 俯冲洋壳熔融形成强烈亏损HREE的太古宙TTG的模式也得到许多科学家的支持(Condie, 1981; Nisbet, 1984; Martin, 1986).

但是，相当一部分研究者并不认同俯冲洋壳熔融可以产生中酸性的弧岩浆岩. 一些科学家提出，俯冲洋壳释放的流体所交代的地幔楔熔融产生弧玄武质岩浆, 然后该岩浆进一步演化形成了安山岩-英安岩-流纹岩(例如, Gill, 1981; Tatsumi等, 1986). 这一观点解释了绝大多数火山弧钙碱性火成岩的成因，并成为20世纪80年代大陆弧安山岩成因的主流学派. 1985年, Rogers等通过对墨西哥Baja加尼福利亚新生代火山岩的研究, 提出了与高热的扩张洋脊俯冲密切相关且强烈亏损HREE与Y、富Sr与MgO的巴哈岩(bajaites)(SiO_2<56.3 wt.%)，认为该岩石的源区类似大多数弧岩浆岩的地幔源区，只是前者的源区中含石榴石. Gromet和Silver(1987)则认为，北美西部白垩纪Peninsular山强烈亏损HREE(Yb=0.22~1.44ppm)的中酸性侵入岩由底侵的玄武质下地壳在增厚(>45km)的条件下熔融形成, 熔融后的榴辉岩相残留体将通过拆沉作用回到地幔中.

Defant和Drummond(1990)在系统总结新生代环太平洋岛弧带岩浆岩之后，提出了俯冲洋壳在榴辉岩相条件下熔融可以形成具有特殊地球化学特征的中酸性岩浆岩, 将其命名为“埃达克岩”. 同时，他们将这种岩石与太古宙TTG进行对比，认为其是太古宙高铝TTG的现代类似物，从而提出太古宙板块构造已经启动, 太古宙地壳生长与俯冲洋壳在榴辉岩相条件的熔融有关(Defant和Drummond，1990；Drummond和Defant, 1990). 自Defant和Drummond(1990)命名埃达克岩之后, 这一新的岩石类型引起了广泛关注. 后续的大量研究集中于俯冲洋壳如何熔融产生埃达克岩、埃达克质岩浆与地幔的相互作用以及埃达克岩的成矿意义等. 在2002年，埃达克岩的术语入选《火成岩的分类和术语词典》(Le Maitre，2002). Martin等(2005)曾经将埃达克岩区分为高硅和低硅两种类型，认为高硅型是板片熔体与地幔楔之间相互作用的产物，低硅型是由板片熔体交代的地幔再熔融所形成，并且认为低硅埃达克岩的SiO_2可以小于56.0wt.%，有的甚至接近50.0wt.%. 按照Martin等(2005)的标准，埃达克岩的命名地埃达克岛的埃达克岩都被划归为低硅埃达克岩，Baja加尼福利亚的巴哈岩也被归为了低硅埃达克岩. 但实际上，埃达克岛的埃达克岩并不含橄榄石，其岩浆与地幔橄榄岩并不平衡，不应直接来自地幔熔融，而更可能是板片熔体与地幔反应的产物(Kay, 1978). 另外, 巴哈岩是一种来由地幔熔融产生的含橄榄石的高镁安山岩(Rogers等, 1985). 因此, 本文并不赞同低硅埃达克岩的划分方案中将岩石范围扩展到中基性(SiO_2<56.0wt.%)的地幔熔体(Martin等，2005)，更趋向其原始定义中将岩石范围定义为中酸性(SiO_2≥56.0wt.%)岩石，即并不能直接来自地幔超镁铁质岩石熔融的长英质岩石(Defant和Drummond, 1990).

自埃达克岩的概念提出之后，那些与俯冲洋壳熔融形成的埃达克岩具有类似岩石地球化学特征，但又不是由俯冲洋壳熔融形成的中酸性岩浆岩的成因和成矿也备受关注(例如，Atherton和Petford, 1993; Petford和Atherton, 1996; 张旗等, 2001; Xu等, 2002; Chung等,

2003; Gao等, 2004; Hou等, 2004; Wang等, 2005, 2006a, 2006b, 2007a, 2007b, 2008; Castillo, 2006). 一些研究者针对具有类似岩石地球化学特征的中酸性岩石, 也提出了高Ba-Sr花岗岩类(Tarney和Jones, 1994)、埃达克质(adakitic(Yumul等, 2000)或adakite-like(Harris等, 1996))岩、“C型埃达克岩”(张旗等, 2001)或“地壳型(crustally-derived)埃达克岩”(Sheppard等, 2001)、富Sr安山岩(Conrey等, 2001)以及高Sr/低Y型中酸性火成岩(葛小月等, 2002; Zeng等, 2011)等. 如前面所述, 本文将那些与俯冲洋壳熔融形成的埃达克岩具有类似岩石和地球化学特征中酸性岩浆岩称为“埃达克质岩”.

3 新生代汇聚板块边缘埃达克质岩成分特征与岩浆起源

大量资料表明, 新生代埃达克质岩几乎全分布在汇聚板块边缘(图1a), 如洋内弧、大陆弧、陆缘岛弧(例如, Defant和Drummond, 1990; Gutscher等, 2000)和大陆碰撞带(例如, Chung等, 2003; Hou等, 2004), 只有极少数分布在陆内环境(如青藏高原北部羌塘、可可西里等地(Wang等, 2005, 2008)), 而且相当一部分埃达克岩与铜、金、钼等矿床密切共生(图1a和1b).

3.1 新生代洋内弧埃达克岩

洋内弧是由一个大洋岩石圈向另外一个大洋岩石圈之下俯冲所形成的. 新生代洋内弧埃达克岩主要分布在阿留申、伊豆-小笠原-马里亚纳(IBM)、马来西亚-印度尼西亚、所罗门-斐济-汤加等岛弧(例如, Kay, 1978; Yogodzinski等, 1995; Yogodzinski和Kelemen, 1998; König等, 2007; Danyushevsky等, 2008; Falloon等, 2008; Schuth等, 2009; Coldwell等, 2011; Li Y B等, 2013)(图1). 这些埃达克岩包含有安山岩-英安岩-花岗斑岩等岩石, 形成于43.1~2.5Ma, 具有相对变化较大的SiO_2含量(55~74wt.%)(图2). 洋内弧埃达克岩具有相对低的全碱含量(2.0~7.0wt.%)(图2a)和K_2O含量(<3.0wt.%)(图2b), 属于低钾拉斑-钙碱性系列. 岩石显示了轻稀土富集、重稀土亏损, 轻/重稀土分异明显, 以及正Sr异常无Eu异常和Nb、Ta亏损(图3a和3b), 较低的K_2O/Na_2O比值、Th含量(图4a), 明显亏损的Sr-Nd同位素特征(ε_{Nd}=+5~+12, $^{87}Sr/^{86}Sr$=0.7028~0.7042)(图4b). 除了Sr-Nd同位素组成外, 西南太平洋所罗门群岛中新世洋内弧埃达克岩还具有类似玄武质洋壳的Hf同位素组成(ε_{Hf}=+12~+14)(Schuth等, 2009). 因此, 新生代洋内弧埃达克岩基本显示了与俯冲玄武质洋壳类似的Sr-Nd-Hf同位素组成, 暗示了俯冲玄武质洋壳组分的主要贡献. 但是, 俯冲板片产生的岩浆在上升过程中, 必然会受到地慢楔的混染, 可能会导致岩石的MgO含量、$Mg^{\#}$($100\times Mg^{2+}/(Mg^{2+}+Fe^{total})$)增高(图5a)(例如, Stern和Kilian, 1996; Rapp等, 1999).

洋内弧埃达克岩通常被解释为俯冲的大洋板片在石榴石稳定的温压条件下发生部分熔融, 产生高Sr、低Y、亏损重稀土元素的熔体, 熔体在穿过上覆地幔楔时, 可以与其发生反应, 形成具有高Mg、Cr和Ni等特征的熔体, 随后喷出地表或侵入洋内弧地壳形成埃达克岩(例如, Kay, 1978; Yogodzinski等, 1995; Yogodzinski和Kelemen, 1998; König等, 2007). 然而, 这些埃达克岩仅在部分洋内弧出现, 并非广泛分布, 这主要归因于俯冲洋壳的部分熔融是在特定条件下才会发生. Defant和Drummond(1990)通过统计洋内弧和陆缘岛弧背景下埃达克岩形成和俯冲的洋壳年龄提出, 年龄≤25Ma可能是俯冲板片发生部分熔融的必要条件. Peacock等(1994)通过实验岩石学和数值模拟提出, 只有年龄≤5Ma的俯冲板片才会发生部分熔融, 然而这无法解释一些埃达克岩相关的俯冲洋壳年龄为10~45Ma. Gutscher等(2000)认为, 平坦俯冲可以使俯冲大洋板片尽可能长时间地留在地幔顶部, 使得较老的俯冲大洋板片(即使年龄达到50Ma)也有足够的时间被周围的地幔加热到可以发生部分熔融的温度. Yogodzinski等(2001)认为俯冲板片的熔融不仅是由板片年龄决定, 俯冲板片的几何形态也具有重要的影响, 提出在阿留申岛弧东端靠近勘察加半岛区域的埃达克岩的形成与撕裂板片边缘的熔融有关. 此外, 根据阿留申弧东、西段的俯冲板片年龄和速度的差异, 数值模拟结果认为西段出现板片熔融是因为板片较为年轻且俯冲速度较慢(Lee和King, 2010). 因此, 决定俯冲大洋板片是否发生部分熔融的因素包含有俯冲洋壳的年龄、速率和几何形态.

3.2 新生代大陆弧埃达克岩

大陆弧是大洋岩石圈向大陆岩石圈之下俯冲时在大陆边缘形成并且还没有同大陆分离的火山弧. 大陆弧是新生代埃达克岩的主要分布位置, 在太平洋东岸

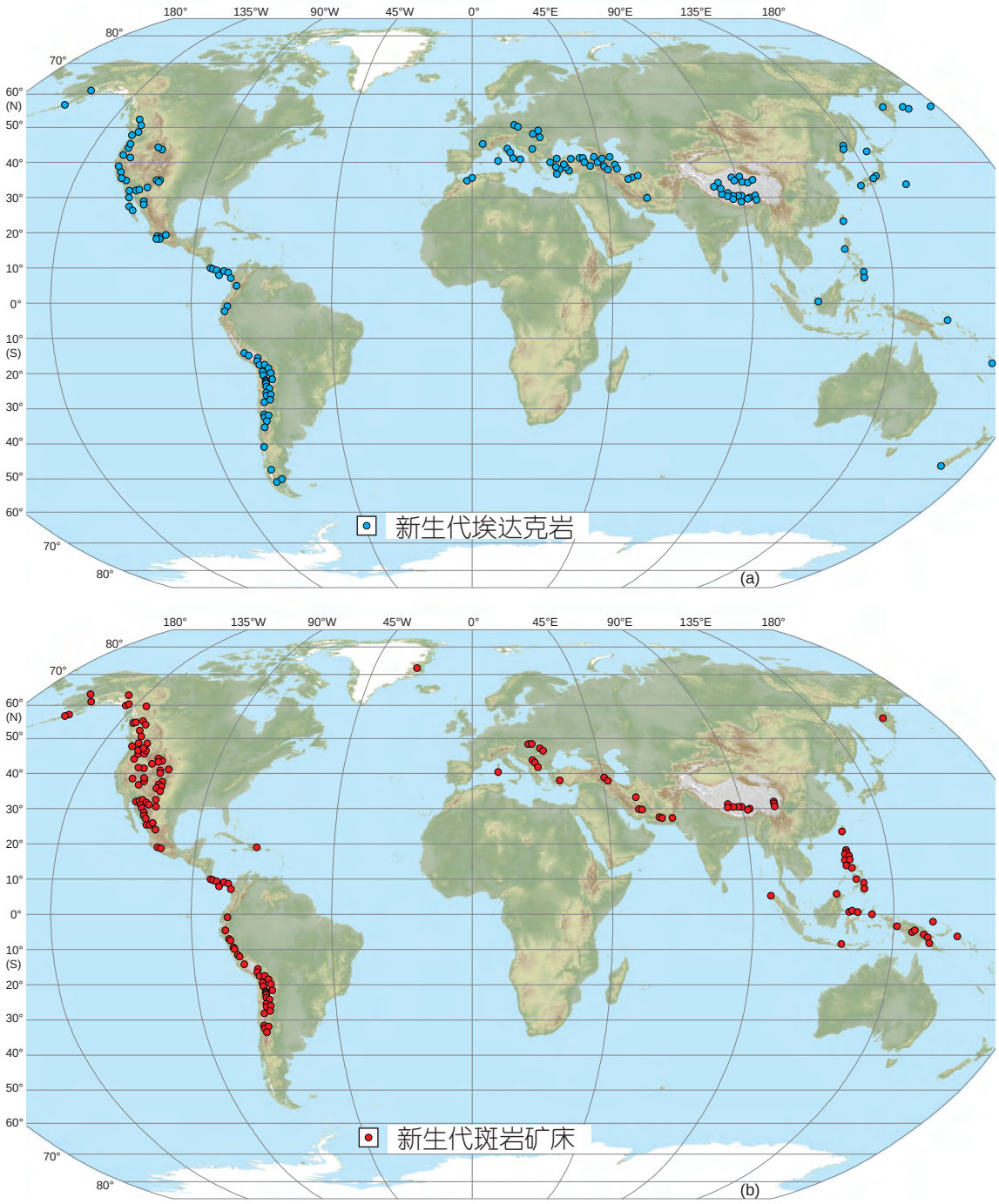

图 1　全球新生代埃达克岩(a)和斑岩矿床(b)的分布

全球新生代埃达克岩资料来自文献(Defant和Drummond, 1990; Stern和Kilian, 1996; Castillo等, 1999; Gutscher等, 2000; Yogodzinski等, 2001; Chung等, 2003; Hou等, 2004; Wang等, 2005, 2008; Macpherson等, 2006; Richards和Kerrich, 2007; Falloon等, 2008; Chiaradia, 2009; Goss等, 2013; Gazel等, 2015; Pang等, 2016; Ou等, 2017及其所引参考文献), 斑岩矿床资料自文献(Hou和Cook, 2009; Lee和Tang, 2020及其所引参考文献)

的美洲大陆边缘广泛分布(图1), 包括智利、秘鲁、厄瓜多尔、哥伦比亚、哥斯达黎加、巴拿马、墨西哥、加拿大等地(例如, Gutscher等, 2000; Beate等, 2001; Oyarzun等, 2001; Samaniego等, 2002; Bourdon等,

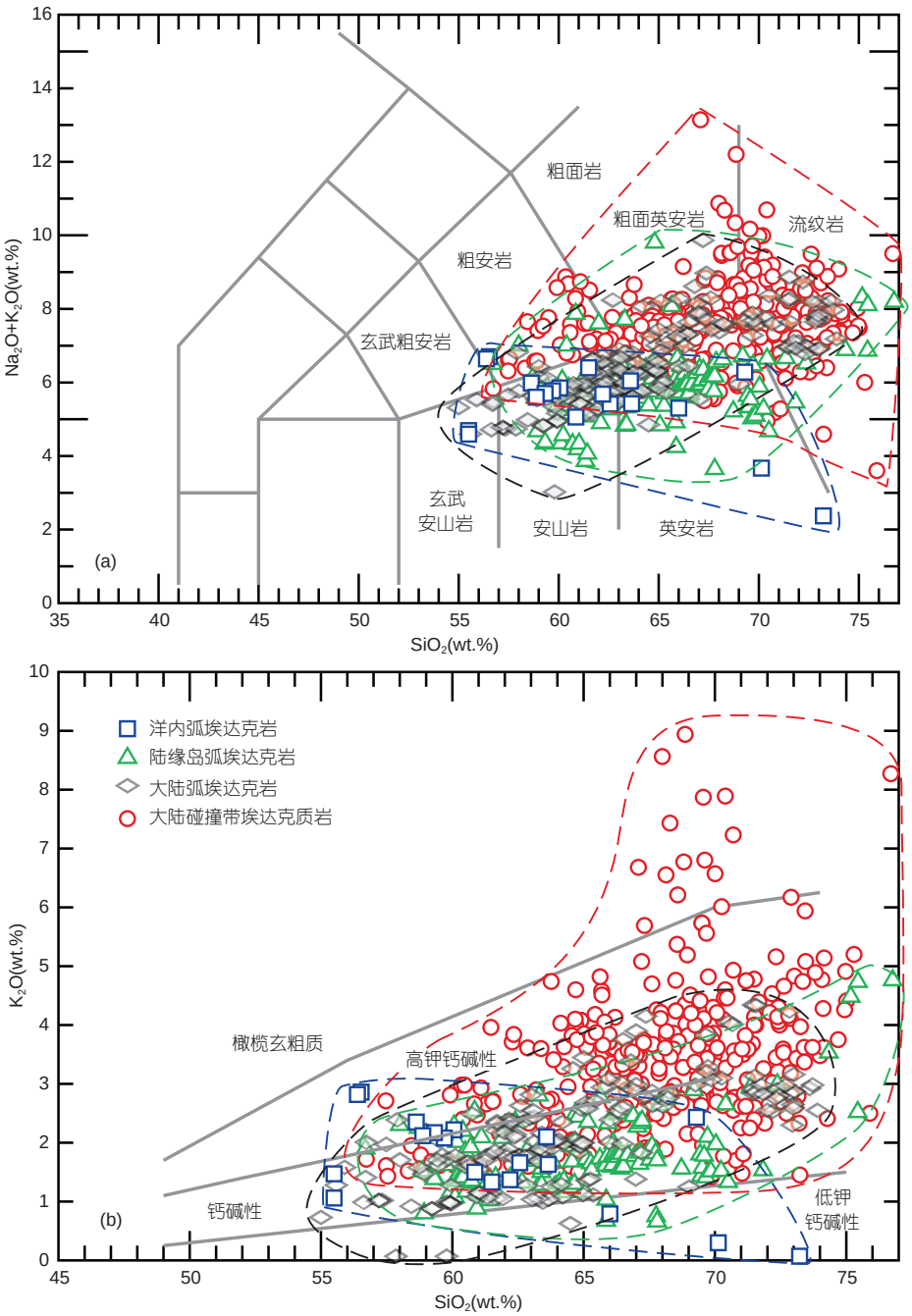

图 2　全球新生代汇聚板块边缘(洋内弧、大陆弧、陆缘岛弧和陆陆碰撞带)埃达克岩的主量元素特征

(a) SiO_2-K_2O+Na_2O图(Le Bas等, 1986). (b) SiO_2-K_2O图(Peccerillo和Taylor, 1976). 数据来源: 洋内弧埃达克岩(n=19): Kay(1978)、Yogodzinski等(1995)、Yogodzinski和Kelemen(1998)、Falloon等(2008)、Danyushevsky等(2008)、Schuth等(2009)、Li等(2013). 陆缘岛弧埃达克岩(n=128): Sajona等(1993, 1994, 1996)、Castillo等(1999, 2007)、Macpherson等(2006)、Coldwell等(2011)、Breitfeld等(2019)、Pineda-Velasco等(2018)、Hu等(2019)、Payot等(2007). 大陆弧埃达克岩(n=167): Reich等(2003)、Bourdon等(2002, 2003)、Petrone和Ferrari(2008)、Castillo(2008)、Ickert等(2009)、Rooney等(2011)、Chiaradia(2009)、Oyarzun等(2001)、Rodríguez等(2007)、Rabbia等(2017)、Beate等(2001)、Martínez-Serrano等(2004). 新生代碰撞带埃达克质岩(n=346): Chung等(2003)、Hou等(2004)、Wang等(2005)、Gao等(2007)、Guo等(2007)、Jahangiri(2007)、Zeng等(2011)、Zheng等(2012)、Jiang等(2014)、Ma等(2014)、Zhang等(2014)、Long等(2015)、Yang等(2015)、Moghadam等(2016)、Pang等(2016)、Wang等(2016)、Liu等(2017)、Nia等(2017)、Ou等(2017)

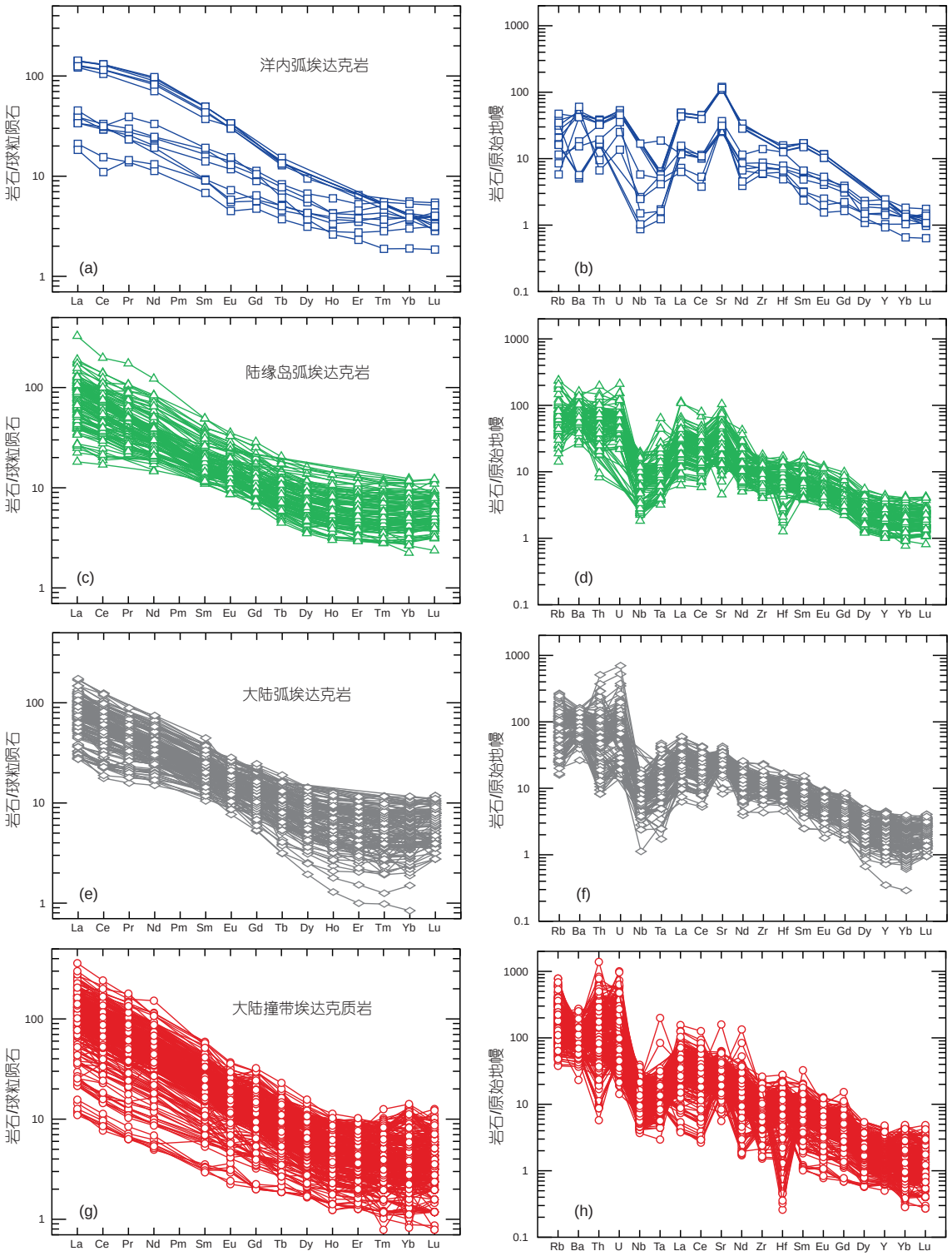

图 3　全球新生代汇聚板块边缘(洋内弧((a)和(b))、陆缘岛弧((c)和(d))、大陆弧((e)和(f))和陆陆碰撞带((g)和(h))埃达克岩的稀土和微量元素特征

资料来源同图2. 球粒陨石和原始地幔标准化数值引自Sun和McDonough(1989)

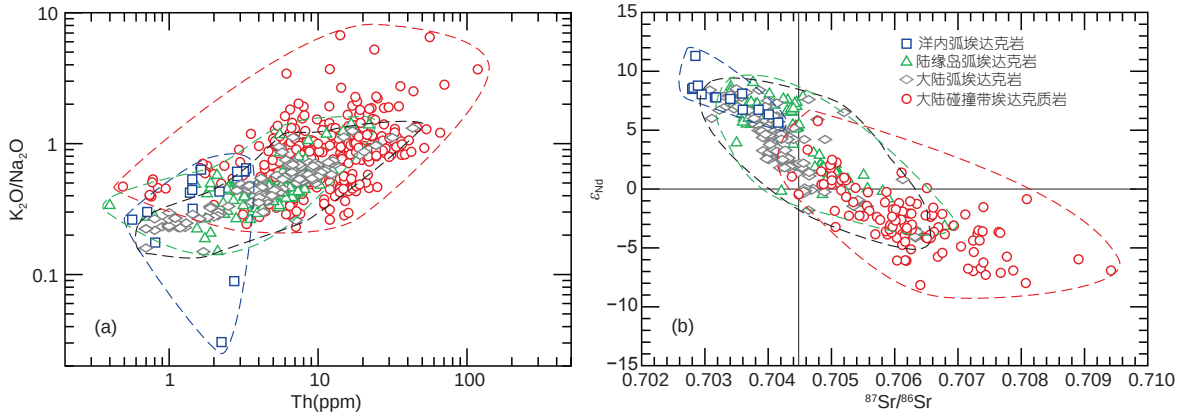

图 4　全球新生代汇聚板块边缘(洋内弧、大陆弧、陆缘岛弧和陆陆碰撞带)埃达克岩的(a)Th-K_2O/Na_2O和(b)Sr-Nd同位素特征

资料来源同图2

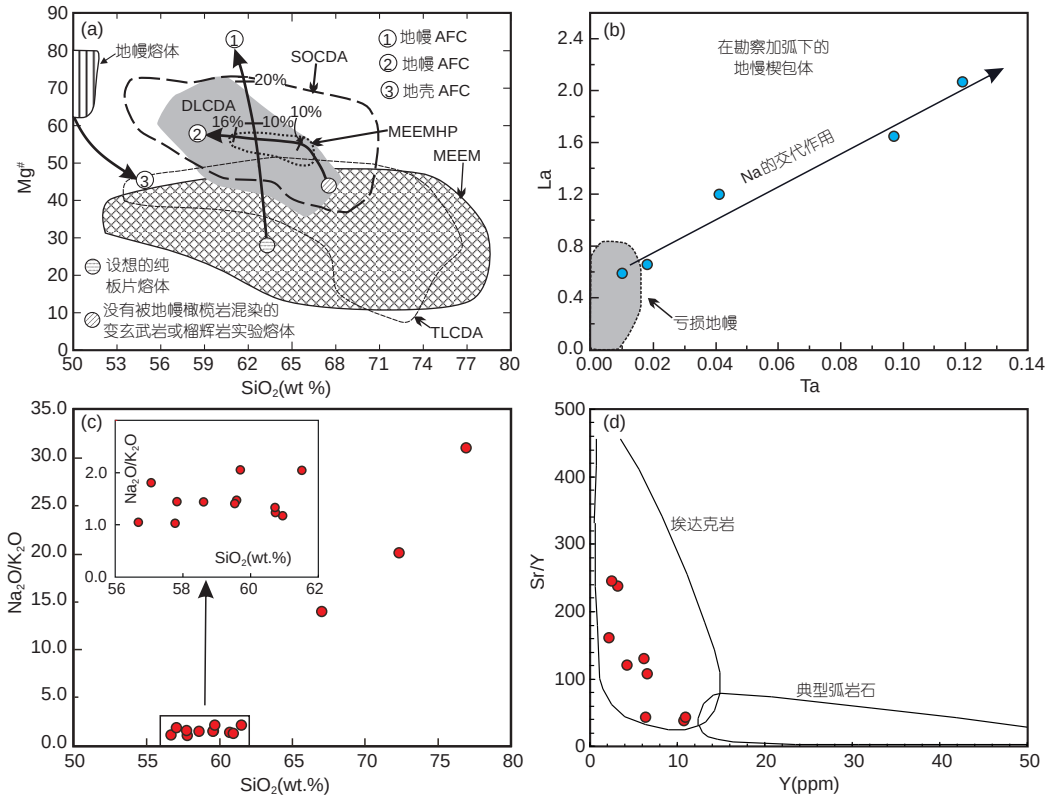

图 5　板片熔体与地幔楔的相互作用

(a) 实验熔体、埃达克岩的SiO_2与$Mg^{\#}$图解(Wang等, 2006a, 2006b). 板片熔体在上升过程中受到地幔混染, 导致$Mg^{\#}$升高. 实验熔体: MEEM-变玄武岩和榴辉岩的实验熔体(1~4.0GPa); MEEMHP-被橄榄岩混染的变玄武岩和榴辉岩熔体. 埃达克岩: TLCDA-增厚下地壳熔融形成的埃达克岩; DLCDA-拆沉下地壳熔融形成的埃达克岩; SOCDA-俯冲洋壳熔融形成的埃达克岩. (b) 勘察加弧下地幔楔橄榄岩包体的Ta和La变化图解(Defant和Kepezhinskas, 2001; Defant等, 2002). La容易在含水流体中迁移, 但Ta并不在含水流体中迁移; La和Ta的相关性说明了含水流体的交代并不是弧下地幔唯一的过程, 富Na板片熔体的交代也广泛存在. (c)和(d) 菲律宾弧下地幔包体(来自新生代火山岩)的橄榄石中含水富硅熔体包裹体SiO_2与Na_2O/K_2O和Y与Sr/Y图解. 资料来源为Schiano等(1995)

2003; Kay等, 1993; Reich等, 2003; Rodríguez等, 2007; Goss和Kay, 2006; Coldwell等, 2011; Chiaradia, 2009; Gazel等, 2015). 新生代大陆弧埃达克岩包含安山岩-英安岩-流纹岩-花岗闪长斑岩等岩石, 形成于50~0.1Ma, 岩石整体上与陆缘岛弧埃达克岩相似, 例如, 具有相对高的且变化较大的SiO_2含量(54.0~74.0wt.%)(图2), 相对高的全碱含量(3.0~10.0wt.%)(图2a)和K_2O含量(0.1~4.5wt.%)(图2b), 绝大多数属于中钾-高钾钙碱性系列. 大陆弧埃达克岩富集LREE、亏损HREE, 轻/重稀土分异明显, 无明显Eu异常, 正Sr到负Sr异常(图3e~3f), 以及略高的K_2O/Na_2O比值、Th含量(图4a). 大陆弧埃达克岩显示变化较大的从亏损到富集的同位素特征(ε_{Nd}=−4~+8.5, $^{87}Sr/^{86}Sr$=0.7030~ 0.7064)(图4), 暗示了其源区组成的复杂性. 中美洲哥斯达黎加、巴拿马弧上新世以来埃达克岩具有相对低的近似MORB的Li、Fe和Zn同位素组成, 其中δ^7Li=1.4~4.2‰、δ^{56}Fe=+0.063~+0.133‰和δ^{66}Zn=+0.23~+0.33‰(Tomascak等, 2000; He等, 2017; Huang等, 2018)暗示了洋壳组分的贡献. 北美洲Mt. Shasta弧<0.1Ma火山岩中具埃达克质特征的熔融包裹体近似MORB的极低B含量(0.71.6ppm)和较低且变化较大的δ^{11}B值(−21.3~−0.9‰), 暗示其来源于持续脱水后的残余热板片部分熔融(Rose等, 2001).

大陆弧(尤其是南美的安第斯山)涉及到正常洋壳、无震海岭或大洋高原、扩张洋脊的俯冲以及俯冲侵蚀或地壳被加厚、拆沉等众多因素的影响. 因此, 产于该背景中埃达克岩的成因较为复杂, 其源区物质包括俯冲的正常洋壳、无震海岭或大洋高原及其携带的沉积物、俯冲扩张洋脊或撕裂板片的边缘(例如, Stern和Kilian, 1996; Gutscher等, 2000; Abratis和Wörner, 2001; Beate等, 2001; Samaniego等, 2002; Bourdon等, 2003; Martínez-Serrano等, 2004; Breitsprecher和Thorkelson, 2009; Gazel等, 2015; Bourgois等, 2016; 王强等, 2020)、被俯冲侵蚀带入到地幔深处的俯冲上盘物质(Goss和Kay, 2006)和增厚或拆沉下地壳等的熔融(Kay和Mahlburg, 1991, 1993; Kay等, 1993; Kay和Mpodozis, 2001; Atherton和Petford, 1993; Petford和Atherton, 1996; Castillo, 2008; Ickert等, 2009; Coldwell等, 2011).

3.3 新生代陆缘岛弧埃达克岩

新生代陆缘岛弧埃达克岩主要分布在亚洲东部的千岛群岛、日本、琉球、吕宋-菲律宾、马来西亚-印度尼西亚等地(例如, Sajona等, 1993, 1994, 1996; Castillo等, 1999, 2007; Macpherson等, 2006; Payot等, 2007; Coldwell等, 2011; Breitfeld等, 2019; Kamei等, 2009; Pineda-Velasco等, 2018; Hu等, 2019)(图1), 包含有安山岩-英安岩-流纹岩-花岗闪长岩等岩石, 形成于17~0.3Ma. 相比于洋内弧埃达克岩, 新生代陆缘岛弧埃达克岩具有相似的SiO_2含量(57~77wt.%)(图2), 相对高的全碱含量(3.5~10.0wt.%)(图2a)和K_2O含量(0.5~5.0wt.%)(图2b), 绝大多数属于中钾-高钾钙碱性系列. 新生代陆缘岛弧埃达克岩轻稀土富集, 重稀土亏损, 轻-重稀土分异明显, 无明显Eu异常, 负-正Sr异常(图3c和3d), 略高的K_2O/Na_2O比值、Th含量(图4a), 显示从富集到亏损的Sr-Nd同位素特征(ε_{Nd}=−3~+9, $^{87}Sr/^{86}Sr$=0.7034~0.7068), 部分与洋内弧埃达克岩的Nd-Sr同位素成分叠加, 另外一部分明显不同于洋内弧埃达克岩的Nd-Sr, 显示了富集的Nd-Sr同位素组成(图4b). 因此, 除了俯冲的玄武质洋壳组分的贡献之外, 俯冲沉积物、大陆弧地壳组分的贡献或后期的分离结晶和地壳混染过程可能也在新生代陆缘岛弧埃达克岩的形成中发挥了作用. 如日本弧西南部的晚新生代(2Ma)的埃达克质岩石(富Sr安山岩和英安岩), 其母岩浆是洋脊俯冲过程中俯冲玄武质洋壳部分熔体和沉积物部分熔体混合形成的, 随后母岩浆在地壳岩浆房中发生分离结晶, 最终喷发出地表形成埃达克质火山岩(Pineda-Velasco等, 2018). 日本弧新生代(包括第四纪)埃达克岩主要出现在西南部地区, 主要是因为该区域与年轻的洋壳(即菲律宾海板块)的俯冲(Morris, 1995; Peacock和Wang, 1999)或九州-帕劳海岭俯冲导致的板片撕裂(Pineda-Velasco等, 2018)有关. 根据上述实例分析, 可见陆缘岛弧的形成机制有两种(徐义刚等, 2020). 一是随着大洋岩石圈的连续俯冲将洋内弧迁移到大陆边缘发生增生造山, 二是大洋岩石圈向大陆岩石圈之下俯冲过程中由于弧后扩张等作用导致原本位于大陆边缘的大陆弧从大陆分离出来.

3.4 新生代大陆碰撞带埃达克质岩的特征与成因

新生代大陆俯冲-碰撞带埃达克质岩主要分布在欧亚大陆内部的特提斯构造域内, 包括喀尔巴阡-潘诺尼亚地区(例如, Seghedi等, 2004)、希腊地区(例如, Marchev等, 2013)、土耳其-伊朗地区(例如, Dokuz等,

2013; Jahangiri, 2007; Moghadam等, 2016; Nia等, 2017; Omrani等, 2008; Pang等, 2016; Topuz等, 2011), 以及喜马拉雅-青藏高原地区(例如, Chung等, 2003, 2005, 2009; Hou等, 2004, 2012; Wang等, 2005, 2008; Gao等, 2007; Guo Z等, 2007; Zeng等, 2011; Zheng等, 2012; Jiang等, 2014; Ma等, 2014; Zhang等, 2014; Long等, 2015; Liu等, 2017; Ou等, 2017), 包含有花岗闪长岩-花岗岩-花岗闪长斑岩-英安岩-流纹岩等岩石, 形成于56~2.5Ma. 碰撞带新生代埃达克岩中SiO_2含量(57.0~77.0wt.%)与新生代弧埃达克岩类似(图2), 但具有相对高的全碱含量(3.5~13wt.%)(图2a)、K_2O含量(1.3~9.0wt.%)(图2b), 以及K_2O/Na_2O比值、Th含量(图4a), 岩石属于中钾-高钾钙碱性-橄榄玄粗质系列, 与新生代弧环境中的埃达克质岩略微不同. 新生代碰撞带埃达克质岩微量元素上以显著的轻/重稀土分异为特征, 无明显Eu异常, 正Sr到负Sr异常(图3g和3h), 在新生代埃达克质岩中显示了较富集的同位素特征(ε_{Nd}=−8~+6, $^{87}Sr/^{86}Sr$=0.7044~0.7094)(图4b). 这和碰撞带多种物源参与埃达克质岩形成有关, 包括增厚下地壳或俯冲陆壳, 组分包括古老地壳物质(例如俯冲陆壳或者加厚古老下地壳)、新生地壳或残留的洋壳等, 形成的动力学机制包括大陆俯冲、板片断离或岩石圈拆沉等. 其中, 特提斯-青藏高原碰撞带的新生代埃达克质岩主要被认为与碰撞加厚下地壳部分熔融有关.

4 新生代弧环境埃达克岩的共生岩石组合及板片熔体交代作用

玄武岩-安山岩-英安岩-流纹岩组合是典型的同时也是分布最广的弧岩浆岩组合, 其形成一般认为与俯冲流体交代的地幔楔橄榄岩熔融产生玄武质岩浆及其后续的演化(如地壳混染和分离结晶)过程有关(例如, Gill, 1981; Tatsumi等, 1986). Defant和Drummond(1990)最早在提出埃达克岩的概念时指出, 埃达克岩很少与玄武岩、玄武安山岩共生. 后来, 他们发现拉丁美洲和北美的大陆弧地区一些新生代粗面玄武岩-橄榄玄粗岩岩石与埃达克岩共生, 并且这些岩石具有高Nb(>20ppm)含量或Nb亏损不明显的特征, 将此称为“高Nb玄武岩”(Defant等, 1991, 1992). 一些研究者也进一步报道了菲律宾、勘察加弧、北美下加利福利亚和南美厄瓜多尔“富Nb岛弧玄武岩”(Nb=7~16ppm, Na/La比值>0.5)(Sajona等, 1993, 1996; Kepezhinskas等, 1997; Defant和Kepezhinskas, 2001; Defant等, 2002; Bourdon等, 2003). 这些弧环境中“高Nb玄武岩”或“富Nb岛弧玄武岩”普遍被认为与俯冲板片熔体交代的地幔熔融有关(Sajona等, 1993, 1996; Kepezhinskas等, 1997; Defant和Kepezhinskas, 2001; Defant等, 2002). 另外, 在洋脊俯冲的伸展环境中, 有时候也出现埃达克岩与一些具有洋岛玄武岩(OIB)或MORB地球化学特征的玄武岩共生的现象(Cole和Stewart, 2009; Thorkelson等, 2011; Tang等, 2012). 洋岛型玄武岩主要来自深部地幔的熔融, 而洋中脊型玄武岩可能主要来自上涌软流圈的减压熔融或亏损大洋岩石圈地幔与上涌软流圈相互作用(Thorkelson等, 2011; Tang等, 2012).

在新生代弧中, 除了上述玄武质岩石外, 埃达克岩常常会与高镁或镁质安山岩共生. 高镁安山岩一般包括四类: 埃达克型高镁安山岩、Piip型系列或赞岐岩类、巴哈岩系和玻安岩等(唐功建和王强, 2010). 新生代埃达克型高镁安山岩主要出现在阿留申弧(包括埃达克岩的命名地埃达克岛), 是一种富含普通辉石斑晶以及斜长石、普通辉石微晶不含橄榄石的高镁安山岩, 由板片熔体与地幔橄榄岩的相互作用形成(Kay, 1978; Yogodzinski等, 1995). 新生代的Piip型系列或赞岐岩类分别出现在阿留申群岛西段的Piip岛、日本西南中新世Setouchi火山岩带赞岐地区, 二者都含橄榄石、单斜辉石、斜方辉石的安山岩(Tatsumi和Ishizaka, 1981, 1982a, 1982b; Yogodzinski等, 1994; Tatsumi, 2006). 新生代的Piip型系列或赞岐岩类具有类似的MgO含量、稀土微量元素特征, 主要为俯冲沉积物或流体交代地幔橄榄岩的熔融形成(唐功建和王强, 2010). 巴哈岩(bajaite)命名地为墨西哥巴哈(Baja)加利福利亚半岛(Rogers等, 1985; Saunders等, 1987). 下加利福利亚半岛新生代巴哈岩主要为一套含橄榄岩、单斜辉石、斜方辉石、斜长石以及角闪石的高镁安山岩, 岩石主要由俯冲板片熔体交代形成的含角闪石的地幔橄榄岩的熔融形成(Benoit等, 2002; Castillo, 2008; Pallares等, 2007; Maury等, 2009). 玻安岩是一种富含古铜辉石斑晶、玻璃基质和普通辉石微晶且几乎没有斜长石晶体的高镁喷出岩(Kikuchi, 1890; Cameron等, 1979), 具有特征的地球化学特征, 如SiO_2>52wt.%、MgO>8wt.%、TiO_2<0.5wt.%(Le bas, 2000),

具有U型稀土元素分布模式、强烈亏损高场强元素(HFSE)等(唐功建和王强, 2010). 玻安岩普遍被认为由俯冲沉积物流体交代的亏损地幔橄榄岩熔融所形成(Ishizuka等, 2006, 2011; 唐功建和王强, 2010).

弧环境中埃达克岩与其共生岩石组合的新生代典型实例包括: (1) 阿留申群岛西端埃达克质和Piip型高镁安山岩组合(Yogodzinski等, 1994, 1995, 2001; Yogodzinski和Kelemen, 1998); (2) 西南太平洋所罗门群岛、汤加弧和马里亚纳弧埃达克岩-高镁安山岩-玻安岩组合(Schuth等, 2009; Falloon等, 2008; Li Y B等, 2013); (3) 菲律宾、勘察加弧和南美厄瓜多尔的埃达克岩-高镁安山岩-富Nb玄武岩组合(Sajona等, 1993, 1996; Kepezhinskas等, 1997; Beate等, 2001; Bourdon等, 2003); (4) 北美下加利福利亚半岛埃达克岩-巴哈岩-富Nb玄武岩-MORB型拉斑玄武岩组合(Benoit等, 2002)等. 因此, 一些学者提出板片或沉积物熔体的交代作用可以形成一套特殊的岩石组合——埃达克岩-埃达克型高镁安山岩-Piip型高镁安山岩-富Nb玄武岩-玻安山岩等(Defant和Kepezhinskas, 2001; Defant等, 2002). 该组合与俯冲洋壳流体交代地幔楔形成钙碱性玄武岩-安山岩-英安岩-流纹岩的组合明显不同.

板片熔体与地幔楔橄榄岩之间的相互作用有实验和岩石学的证据, 包括: (1) 实验岩石学研究表明, 在1~4GPa条件下实验熔体具有低的$Mg^{\#}$(小于47)(图5a), 但当实验熔体与橄榄岩发生反应后, 熔体的$Mg^{\#}$明显增高(大于47)(Rapp等, 1999; Wang等, 2006a, 2006b); (2) 勘察加弧北部新生代火山岩携带的地幔橄榄岩包体中有富Nb玄武质、埃达克质脉体以及富Na、Sr和高La/Yb的辉石, 并且橄榄岩包体中轻稀土元素与高场强元素含量相关(图5b), 显示弧下地幔经历了来自板片的钠质熔体交代作用(Kepezhinskas等, 1995; Kepezhinskas和Defant, 1996; Defant和Kepezhinskas, 2001; Defant等, 2002); (3) 菲律宾弧下地幔包体(来自新生代火山岩)的橄榄石中含水富硅熔体包裹体显示了富钠的(Na_2O/K_2O=1.03~31.01)埃达克质熔体特征(图5c和5d), 也显示弧下地幔经历了来自板片的钠质熔体交代作用(Schiano等, 1995; Defant和Kepezhinskas, 2001); (4) 实验岩石学研究表明, 自然界新生代埃达克岩具有比玄武岩高压下的实验熔体更低的Na_2O含量(通常小于5wt.%), 这是板片熔体吸收了地幔低钠的矿物而结晶了富钠的角闪石的结果(Xiong等, 2006).

5　埃达克质岩浆产生的岩石学、变质相平衡模拟和高温高压熔融实验制约

5.1　与榴辉岩(或高压麻粒岩)相岩石共生的熔体

俯冲板片熔融形成的埃达克岩与榴辉岩(或高压麻粒岩)相岩石共生等地质现象指示, 地壳岩石在高压下的部分熔融是形成埃达克岩最可能的方式. 近年来, 有一些研究发现了与榴辉岩(或高压麻粒岩)相岩石共生的熔体, 包括: (1) 柴北缘与退变质榴辉岩(或高压麻粒岩)共生的埃达克质脉体和侵入体: 峰期超高压榴辉岩相变质时代为440~430Ma, 共生的埃达克质石英闪长岩-奥长花岗岩形成于446~420Ma, 与榴辉岩折返过程中的减压熔融有关, 部分熔融条件为T=800~950℃和P=1.5~2.0GPa(Chen等, 2012; Yu S Y等, 2015, 2019; Song等, 2014; Zhang G B等, 2015; Zhang L等, 2015); (2) 德国Münchberg地体与退变质榴辉岩共生的埃达克质含黝帘石伟晶岩脉体: 榴辉岩的原岩为洋中脊玄武岩, 峰期变质条件的下限为P=2.0~2.5GPa, T=600~700℃, 变质时代为395~380Ma, 共生的埃达克质含黝帘石伟晶岩脉体的熔体产生温压条件为680℃/2.3GPa到750℃/3.1GPa, 来源于洋壳在深俯冲过程中的部分熔融, 并最终在榴辉岩折返过程中的低温低压(620~650℃/0.9GPa)条件下完全固结(Franz和Smelik, 1995; Liebscher等, 2007); (3) 出露于高压、超高压岩石矿物中的多相固相包裹体: 德国Erzgebirge超高压片麻岩的石榴石中含金刚石多相包裹体(金云母、石英、钠云母、多硅白云母和金红石)形成于超高压条件(在1000℃时候压力(P)>4.5GPa)的含水熔体, 最终在折返至低压条件下完全结晶(Stöckhert等, 2001); 大别超高压榴辉岩的石榴石中多相固相包裹体(具有埃达克质岩的高Sr/Y特征)形成于榴辉岩折返过程中多硅白云母的脱水熔融(Gao等, 2012, 2013; Hermann等, 2013; Zheng和Hermann, 2014); 欧洲中部Bohemian高压麻粒岩的石榴石中的"纳米花岗岩"包裹体形成于变质峰期阶段(T=850~950℃和P=2.0~3.0GPa)的熔融(Ferrero等, 2015). 因此, 野外实例和室内岩相学的证据显示, 榴辉岩相或高压麻粒岩相条件下的部分熔融产生埃达克质熔体的可能性是存在的.

5.2　火成岩中榴辉岩包体及其与埃达克质或TTG岩浆产生的关联

一些火成岩中包含有榴辉岩包体, 可能与埃达克

质或TTG岩浆的产生之间存在着关联, 包括: (1) 徐淮地区早白垩(132~130Ma)埃达克岩中榴辉岩类捕虏体: 榴辉岩的形成温压分别为>1.5GPa、800~1060℃, 榴辉岩和石榴石辉石岩的锆石和金红石年龄为209~132Ma, 暗示埃达克岩寄主岩与包体之间存在成因联系(例如, Xu等, 2006, 2009; 熊伯琴等, 2015); (2) 南非、俄罗斯太古宙(约3.5~2.5Ga)克拉通的金伯利岩中包含的许多榴辉岩捕虏体(例如, MacGregor和Manton, 1986; Ireland等, 1994; Jacob等, 1995; Beard等, 1996; Rollinson, 1997; Snyder等, 1997; Rudnick等, 2000): 地球化学分析表明, 其中低镁榴辉岩为大洋板片俯冲时形成的榴辉岩经历过TTG熔体提取后的残留, 而高镁榴辉岩则是增厚地壳熔融产生TTG后的残留体(弧根堆晶岩)(例如, Horodyskyj等, 2007).

5.3 变质相平衡模拟榴辉岩(或高压麻粒岩)相条件下埃达克质或TTG熔体的产生

最近一些研究通过变质相平衡模拟方法来约束埃达克质或TTG熔体产生的条件(例如, Wang等, 2015, 2017; Palin等, 2016; Johnson等, 2017; 魏春景等, 2017; Ge等, 2018; Hernández-Uribe等, 2020). 太古宙拉斑玄武岩在1.0~1.8GPa和800~950℃时部分熔融形成的熔体与TTG在主微量元素特征上非常类似(Palin等, 2016). 压力太低时, 变基性岩中斜长石大量存在而石榴石和金红石不稳定, 无法形成富集Sr且亏损HREE和高场强元素(HFSE)的熔体. 压力太高时, 一方面俯冲到如此深度时玄武岩基本脱水完成, 能产生的熔体十分有限; 另一方面, 此时Na在单斜辉石(Cpx)中相容性变大, 导致熔体逐渐富K, 与埃达克岩/TTG富Na的性质不符(Schmidt和Poli, 2014). 用大洋中脊玄武岩(MORB)作为初始成分, 通过变质相平衡模拟方法得到TTG形成的最佳条件是1.0~2.5GPa和800~1000℃(魏春景等, 2017). Hernández-Uribe等(2020)通过对原始洋中脊玄武岩和蚀变玄武岩进行变质-熔融相平衡模拟, 发现这些岩石在压力>2.7GPa、温度>820~840℃时, 可产生高SiO_2(68.0wt.%)的埃达克质熔体. 另外, 变质相图确定的早太古宙(3.7Ga)埃达克质TTG(Sr/Y≥100)的形成条件是压力>1.6GPa, 温度800~830℃, 含水2~3wt.%(Ge等, 2018). 可见, 变质相平衡模拟揭示形成埃达克岩的条件是压力>1.0~1.6GPa, 温度为800~1000℃.

5.4 埃达克质熔体产生条件——实验岩石学制约

大量的高温高压熔融实验被用于限定埃达克质岩浆产生条件. 这些资料表明, 埃达克质熔体的产生与基性岩的熔融及源区残留物的组成(石榴石、金红石和斜长石)关系密切(例如, Rapp等, 1991, 1999, 2003; Sen和Dunn, 1994; Rapp, 1995; Rapp和Watson, 1995; Prouteau等, 2001; Skjerlie和Patiño Douce, 2002; Xiong等, 2005; Xiong, 2006; Nair和Chacko, 2008; Qian和Hermann, 2013; Sisson和Kelemen, 2018). 埃达克岩一般亏损HREE和Y元素, 由于HREE与Y相对于石榴石为相容元素. 因此, 部分熔融形成埃达克质岩浆需要岩浆源区残留有石榴石(Defant和Drummond, 1990). 高温高压熔融实验研究显示, 基性岩或榴辉岩部分熔融主要结晶富铁高钙石榴石(Alm>40mol%), 需要压力大于1.0GPa(Rapp, 1995; Rapp和Watson, 1995; Sisson和Kelemen, 2018), 但是只有在大于1.2GPa(相当于地壳40km深处)的条件下熔体才能够与残留石榴石平衡(Rapp, 1995), 并且残留石榴石的比例越高需要的压力越大(图6)(Nair和Chacko, 2008), 产生的熔体强烈亏损HREE与Y(Sen和Dunn, 1994; Rapp和Watson, 1995; Rapp等, 1999). 埃达克岩一般亏损Nb、Ta和Ti等高场强元素, 由于Nb、Ta和Ti相对于金红石为相容元素(Xiong等, 2005; Xiong, 2006). 因此, 部分熔融形成埃达克质岩浆需要岩浆源区残留有金红石(Xiong等, 2005). 在1.0~2.5GPa和900~1100℃条件下含水2%或5%的玄武岩熔融实验中, 发现金红石在含水玄武岩的部分熔融过程中稳定的压力下限为1.5GPa, 而金红石是控制熔体Nb-Ta的负异常所必须的残留相(Xiong等, 2005). 根据金红石出现的最小压力(1.5GPa), 推测俯冲洋壳熔融形成的TTG的深度超过~50km(Xiong等, 2005; Xiong, 2006). 最近, Sisson和Kelemen(2018)发现基性洋壳在1.4~2.8GPa熔融产生的熔体亏损Nb、Ti, 源区残留有石榴石和金红石.

埃达克岩另外一个重要特征是在其稀土、微量元素分配图中常显示正到无Eu异常、Sr异常(图3). 由于Eu与Sr相对于斜长石为相容元素, 因此部分熔融形成埃达克质岩浆需要岩浆源区很少有或没有斜长石. 基性岩的高压熔融实验表明, 无论是脱水(H_2O=1.5~2.0wt.%)、还是含自由水(H_2O=4.0~6.0wt.%)熔融, 斜长石一般>1.3GPa时消失(Sisson和Kelemen, 2018;

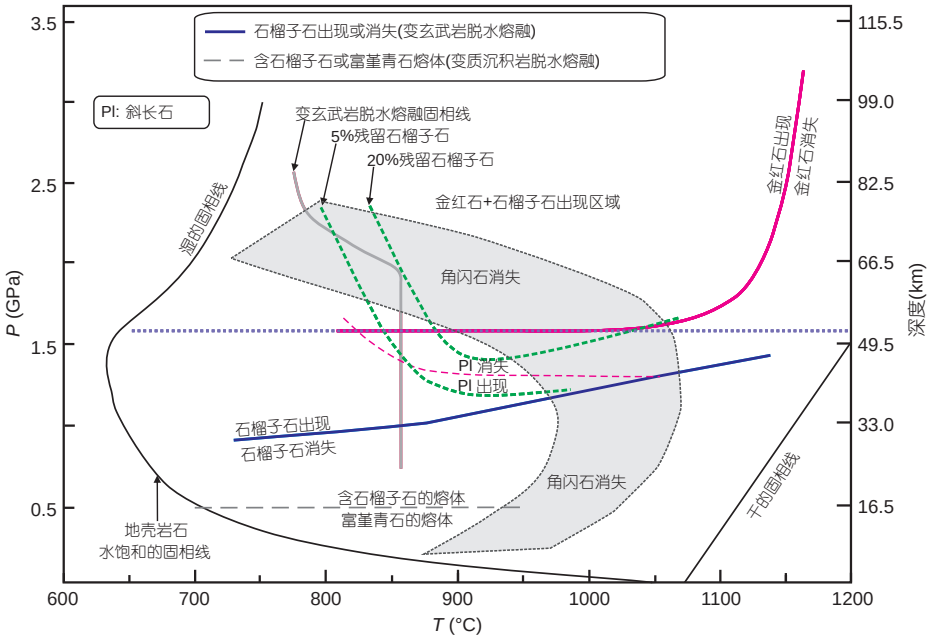

图 6　埃达克质熔体产生的温压条件

修改自Wang等(2016)

Qian和Hermann, 2013), 有时会在>2.2GPa才消失(Rapp和Watson, 1995).

另外, 埃达克质熔体的富钠、富钾特征也普遍受到关注. 基于实验资料的总结, 埃达克质熔体的富钠、富钾特征的影响因素被归结为源岩、水、压力等的影响(Prouteau等, 2001; Skjerlie和Patiño Douce, 2002; 王强等, 2003; Wang等, 2007a; Xiao和Clemens, 2007): 熔融初始物质富钾, 产生的熔体更富钾; 相同的熔融初始物, 贫水熔融导致熔体更富钾, 富水或含自由水的熔融导致熔体富钠; 相同的熔融初始物, 压力越高产生的熔体越富钾. Prouteau等(2001)用洋中脊玄武岩作为初始源岩成分, 在压力1.0~3.0GPa、温度800~1000℃、水含量2.0~10.0wt.%条件下熔融产生了与俯冲带天然埃达克岩一致的主量元素(特别是K_2O、Na_2O)成分.

因此, 结合与榴辉岩或高压麻粒岩密切共生的埃达克质花岗岩或埃达克质“微粒花岗岩”、埃达克岩中榴辉岩或石榴石辉石岩包体、变质相模拟以及高温高压熔融试验的资料, 要解释埃达克质岩亏损重稀土和Nb-Ta-Ti, 以及正到无Eu异常、正Sr异常和K_2O、Na_2O特征, 需要基性岩的源区残留矿物组合为石榴石+金红石, 很少或无斜长石, 压力范围为1.2~3.0GPa, 温度范围是800~1000℃(图6), H_2O的含量范围1.5~6.0wt.%.

6　埃达克质岩与金属成矿

斑岩矿床系统提供了全球75%的Cu、50%的Mo、20%的Au等(Sillitoe, 2010), 对其研究具有极为重要的经济价值和科学意义. 俯冲带是斑岩矿床发育最为密集的地带, 全球新生代斑岩矿床主要出现在环太平洋俯冲带和特提斯构造域(图1b), 与新生代埃达克岩的分布范围重合(图1a), 而且绝大多数成矿母岩体具有埃达克质岩的特征(例如, Thiéblemont等, 1997; Sajona和Maury, 1998; Oyarzun等, 2001; Defant和Kepezhinskas, 2001; Defant等, 2002; 王强等, 2002; Hou, 2010; Loucks, 2014). 目前的主流观点认为, 斑岩矿床是浅成多期次构建的岩浆房顶部流体出溶的结果(Hedenquist和Lowenstern, 1994; Richards, 2003; Sillitoe, 2010; Audétat和Simon, 2012). 尽管并不是所有的埃达克质岩都具有成矿潜力(如Wang等, 2007a, 2007b), 但是, 除了富水、高氧逸度、含S等属性, 埃达克质地球化学特征也已成为判别成矿潜力的重要指标之一(Defant和Kepezhinskas, 2001; Defant等, 2002; 王强等,

2002; Loucks, 2014; Sillitoe, 2018).

众多研究者对埃达克岩与成矿的关系进行了深入研究, 有关埃达克岩有利于成矿的控制因素可以概括为下面几个方面.

(1) 俯冲洋壳熔体高氧逸度导致地幔亲铜元素分解: 埃达克岩之所以有利于成矿, 一个非常重要的原因是板片熔体的高氧逸度(fO_2), 即板片熔体可以携带10000倍于含水流体所携带的Fe_2O_3的量. 携带大量的Fe_2O_3的板片熔体进入到地幔楔时, 将会导致地幔楔橄榄岩fO_2的增高, 以及富集亲铜元素的地幔发生硫化物不饱和的熔融, 从而产生富Au、Cu的弧岩浆以及铜金矿床的形成(Mungall, 2002). 有利于成矿的可能的背景包括年轻洋壳的俯冲、非常缓慢的或斜向汇聚、俯冲板片的停滞(locked)、板片深俯冲(~300km)以及平坦俯冲等(Mungall, 2002).

(2) 岩浆源区(或洋壳)富亲铜元素: 由于铜、金是中度不相容元素, 其在洋壳中的含量(60~125ppm, 平均74ppm)远比地幔(30ppm)和陆壳(27ppm)的平均丰度高. 因此, 洋壳部分熔融形成的岩浆应该具有系统偏高的铜含量, 有利于成矿(Ling等, 2009; 孙卫东等, 2010; Sun等, 2013, 2015; 詹美珍等, 2015).

(3) 埃达克质岩浆富水: 原始富水镁铁质岩浆经历包含角闪石但不含斜长石的结晶分异后产生埃达克质岩浆, 即岩浆中高的水含量能够抑制斜长石的结晶和促进角闪石的分异, 产生的残余岩浆可保持埃达克质岩的地球化学特征, 同时富水. 这一观点在国际成矿岩浆过程研究领域最为流行(例如, Richards和Kerrich, 2007; Richards, 2011; Loucks, 2014; Williamson等, 2016; Sillitoe, 2018), 因为岩浆中富水(>~4%)是成矿的前提(Sillitoe, 2010).

(4) 岩浆高压分离结晶: 深部地壳的岩浆房控制了埃达克质岩浆的形成, 即在较高的压力下, 岩浆会结晶出石榴石和角闪石等(Chiaradia, 2009; Chiaradia和Caricchi, 2017; Lee和Tang, 2020), 这一观点与斑岩矿床更多的产在厚陆壳这一现象相一致(Chiaradia, 2014). 石榴石的分离结晶有可能导致岩浆中氧逸度升高(Tang等, 2019), 有利于成矿(Lee和Tang, 2020).

(5) 增厚的大陆下地壳中角闪石高压下分解: 在俯冲带、碰撞带甚至陆内环境中, 增厚的大陆下地壳中角闪石高压(大于1.2GPa)下分解产生大量富水流体(Kay和Mpodozis, 2001; 王强等, 2002; Hou, 2010), 不仅导致地壳发生熔融, 而且导致岩浆中水含量和氧逸度的升高(Hou, 2010), 从而有利于成矿.

(6) 熔体-地幔作用: 俯冲洋壳(如, Defant和Drummond, 1990)、拆沉下地壳(如, Xu等, 2002, 2006, 2008; Gao等, 2004; Wang等, 2006a, 2006b, 2007a, 2007b)和俯冲大陆地壳(Wang等, 2008; Jiang等, 2014)熔融都可产生埃达克岩, 而且都与金属成矿关系密切(Wang等, 2006a, 2006b, 2007b; 王强等, 2008). 这三种机制的一个共同特征就是埃达克质熔体与地幔发生了相互作用. 因此, 熔体-地幔作用被作为埃达克岩有利于金属成矿的一个有利控制因素(Wang等, 2006a, 2006b, 2007b; 王强等, 2008). 这样, 有利于埃达克岩成矿的构造背景包括大洋俯冲带、大陆碰撞带和陆内伸展区(王强等, 2008).

7 存在问题及未来研究展望

7.1 埃达克质岩形成的构造背景与成因

(1) 前新生代埃达克质岩形成的构造背景复杂性. 埃达克质岩形成的构造背景限制是解决埃达克岩成因的关键第一步. 新生代埃达克质岩的构造背景非常清楚, 主要产出在大洋俯冲带、大陆碰撞带和陆内环境(图1). 但是在前新生代, 也存在有大量的埃达克质岩且相当一部分与金属矿床共生, 如中国东部、秦岭、松潘-甘孜、羌塘、冈底斯、中亚等, 除了一些特殊地区的埃达克质岩形成背景非常清楚之外(如冈底斯侏罗-白垩纪埃达克质岩形成于新特提斯洋俯冲的弧背景中), 大多数地区埃达克质岩的构造背景并不能很好地约束. 比如, 中国东部有大量燕山期的埃达克质岩(张旗等, 2001; Xu等, 2002, 2006, 2009; 王强等, 2002; Wang等, 2004a, 2004b, 2006a, 2006b, 2007a, 2007b; Gao等, 2004; Ling等, 2009; Liu等, 2010; He等, 2011; Ma等, 2012, 2015, 2016; 孙卫东等, 2010; Sun等, 2013, 2015; Li等, 2009; Li X H等, 2013; Xu等, 2014; Yang等, 2014a, 2014b; Dai等, 2017). 但是, 这些岩石究竟是形成在陆内伸展背景, 还是在大陆弧或洋脊俯冲或弧后伸展的背景, 存在激烈争论. 这也导致对其成因认识的不一致. 另外, 有些大陆地区的埃达克质岩浆作用形成于古汇聚板块边缘, 但在时间上晚于所在位置的古板块俯冲, 在形成机制上很可能与增生/碰撞造山带加厚岩石圈的减薄有关, 如大别山早白垩世埃达克质

岩属三叠纪碰撞造山带的再造(王强等, 2001b; Wang等, 2017; Zhao等, 2017). 因此, 要解决一些重要地区前新生代埃达克质岩的成因, 如何更好地约束其形成的构造背景是需要重点解决的问题.

(2) 俯冲带埃达克岩的源区、热源与岩浆产生机制的多样性. 在俯冲带, 埃达克岩的源区物质可能包含俯冲玄武质洋壳、陆壳、俯冲板片沉积物、混杂岩、被侵蚀的俯冲上盘物质等. 对于俯冲板片来说, 可能是年轻或老的洋壳、大洋高原或无震海岭、残留弧脊、扩张洋中脊等(王强等, 2020). 俯冲的方式可能包括板片陡俯冲、平坦俯冲、板片回卷、板片撕裂、俯冲底侵、俯冲侵蚀等(王强等, 2020). 另外, 俯冲带热状态对板片熔融和弧岩浆的产生也有决定性的影响(Zheng, 2019; 徐义刚等, 2020). 一般认为, 除了流体的加入之外, 俯冲板片之上软流圈地幔楔的加热(McGeary等, 1985; Gutscher等, 2000; Frisch等, 2011)、俯冲板片的回卷(rollback)触发软流圈在俯冲板片和地慢楔之间流动带来热(例如, 郑永飞等, 2016; Zheng和Chen, 2016; Zheng和Zhao, 2017; Zheng, 2019; Zheng等, 2020)和俯冲板片的撕裂导致板片之下软流圈上涌带来大量的热(Yogodzinski等, 2001; Rosenbaum等, 2008; 王强等, 2020)对弧岩浆岩的产生有决定性的作用. 以板片回卷为例, 俯冲板片发生回卷, 这时软流圈地幔会加热回卷板片的表面, 使其发生部分熔融产生长英质(包括埃达克质)熔体, 这些熔体与地幔相互作用或交代地幔, 可以形成埃达克岩-高镁安山岩-富Nb玄武质岩石或OIB型玄武岩(例如, Bourdon等, 2003; Tang等, 2010; Zheng等, 2015, 2020; 郑永飞等, 2016; Zheng和Chen, 2016; Zheng和Zhao, 2017; Zheng, 2019; Hao等, 2019; 徐义刚等, 2020; 王强等, 2020). 因此, 俯冲带埃达克岩无论是其源区、热源, 还是岩浆产生机制, 都呈现出多样性. 这种多样性增加了确立俯冲带埃达克岩成因的难度.

(3) 埃达克质岩浆产生的制约. 前面已经提到, 从基性岩高温高压熔融实验的角度来约束埃达克质岩浆的产生条件已经比较成熟. 但存在的一个薄弱点是, 绝大多数基性岩的高温高压熔融实验在研究中所选取的实验初始物质是洋中脊玄武岩型的岩石, 对于具有Nb、Ta亏损的基性岩在什么条件下能够熔融产生埃达克质岩浆, 仍然需要大量的实验工作去证实. 另外, 近年来一些研究也提出了相对低压(1.0~1.2GPa, 即30~40km深处)下地壳岩石的熔融也有可能产生埃达克岩(如华北克拉通(Ma等, 2012, 2015, 2016)和日本弧(Kamei等, 2009)), 并且这些岩石的源岩可能是麻粒岩(例如, Jiang等, 2007)或中酸性岩石(如, Kamei等, 2009). 但是, 也有一些研究者通过实验岩石学资料限定, 得到华北克拉通埃达克岩的主要源区岩石为中钾和高钾基性变质岩, 并通过基性变质岩体系相平衡模拟、长英质熔体TiO_2溶解度、埃达克质岩石Nb/La与La/Yb的相关性等研究, 论证出大别、胶东和华北克拉通北缘许多埃达克质岩石的源区存在残留金红石, 岩浆形成深度超过50km(熊小林等, 2011). 因此, 中酸性岩究竟是否能够产生埃达克岩浆, 以及在何种条件下能够产生这种岩浆, 还需要开展以中酸性岩为初始物质的大量的高温高压熔融实验来约束. 还有, 一些研究者将埃达克岩范围扩大到了SiO_2小于56wt.%的岩石, 甚至把地幔来源的巴哈岩也划归了埃达克岩(即所谓的“低SiO_2埃达克岩”), 并提出低硅埃达克岩可以直接来自地幔橄榄岩的熔融(例如, Martin等, 2005). 但已有的橄榄岩的实验熔体资料显示, 在含自由水的条件下, 橄榄岩主要熔融产生玄武岩, 只产生极少量高镁安山质熔体(SiO_2<57wt.%, MgO>6.0wt.%)(图7). 新生代火山弧和碰撞带埃达克岩的较高的SiO_2(>55wt.%)和较低的MgO(<6.0wt.%)(图2和7), 显示这些岩石不可能直接来自地幔橄榄岩的熔融. 除了地幔橄榄岩, 地幔中其他岩石(如辉石岩)能否产生埃达克质岩浆, 也需要高温高压实验的验证.

(4) 埃达克质岩浆的演化. 尽管大量的研究显示基性岩石的高压(>1.2GPa, 相当于地球40km深处)熔融可以产生埃达克岩(图6). 但是, 来自地壳深处的埃达克质岩浆产生后, 从岩浆源区迁移到最后岩浆喷发或就位期间经历什么样的演化过程(例如, 分离结晶、岩浆混合、AFC或MASH(熔融、混染、贮存、均匀化)等), 对最终埃达克岩的形成也至关重要. 有些研究者提出, 地壳混染与分离结晶、高压分离结晶、岩浆混合都有可能形成埃达克岩(如, Castillo等, 1999; Müntener和Ulmer, 2006; Macpherson等, 2006; Guo F等, 2007; Streck等, 2007; Li等, 2009; Li X H等, 2013; Dai等, 2017). 特别是, 近年来的研究发现, 岩浆在地壳内以低储存温度的“晶粥体”而不是高温的“岩浆房”形式进行储存和演化, “晶粥体”可以在冷的中上地壳能够有效维系较长的热寿命, 这对岩浆储库的生长和演

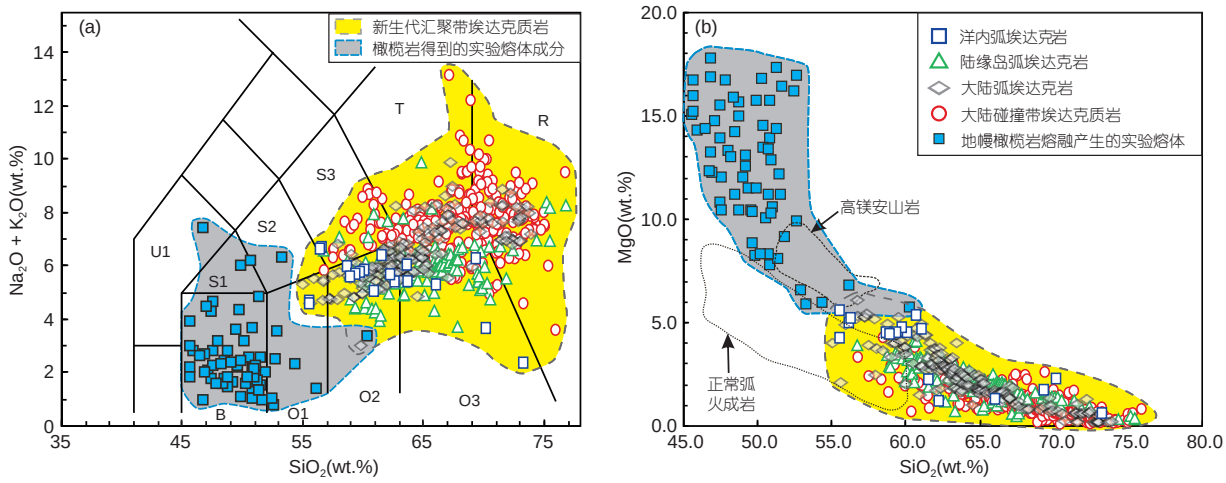

图 7　橄榄岩发生熔融的实验熔体成分与新生代埃达克岩的成分对比

(a) SiO_2与Na_2O+K_2O图解; (b) SiO_2与MgO图解. U1, 碱玄岩; B, 玄武岩; O1, 玄武安山岩; O2, 安山岩; O3, 英安岩; S1, 粗面玄武岩; S2, 玄武粗安岩; S3, 粗安岩; T, 粗面岩/粗面英安岩; R, 流纹岩. 橄榄岩发生熔融的实验熔体成分引自Hirose和Kushiro(1993)、Baker和Stolper(1994)、Baker等(1995)、Hirose和Kawamoto(1995)、Kushiro(1996)、Hirose(1997)、Hirose和Kushiro(1998). 正常弧火山岩和高镁安山岩成分范围引自McCarron和Smellie(1998)

化至关重要(Cashman和Giordano, 2014; Bachmann和Huber, 2016; Edmonds等, 2019; Sparks等, 2019). 比如, 最近的研究显示, 埃达克岩中与早期结晶的角闪石平衡的熔体为埃达克质岩, 但是与晚期结晶的角闪石平衡的熔体并不具有埃达克质岩的特征(Tang等, 2017). 因此, 埃达克质岩浆产生后的长距离迁移、演化过程, 仍然是当前国际地质研究中一个非常薄弱的环节.

7.2　榴辉岩或高压麻粒岩相变质作用与埃达克质熔体产生的关联

前面已经介绍了埃达克质熔体结晶产物与柴北缘都兰榴辉岩、Münchberg地体榴辉岩和大别超高压榴辉岩密切共生. 在上述三个实例中, 除了Münchberg地体埃达克质岩石被认为可能是变质峰期的熔融产物(Franz和Smelik, 1995; Liebscher等, 2007)之外, 柴北缘埃达克岩、大别山高Sr/Y的"纳米花岗岩"都是超高压变质岩在折返过程中熔融产生的(例如, Chen等, 2012; Song等, 2014; Zheng和Hermann, 2014; Zhang G B等, 2015; Zhang L等, 2015; Gao等, 2012, 2013). 早前也有报道俄罗斯白海地区太古宙榴辉岩与埃达克质TTG共生的现象(Mints等, 2010, 2014), 但最新的资料显示, 与榴辉岩伴生的TTG片麻岩原岩形成于3.5~2.6Ga, 与区域内榴辉岩相变质事件(~1.90Ga)无成因联系(Yu H L等, 2019). 最近也有报道, 一些中三叠世(228~219Ma)淡色花岗质脉体与苏鲁将军山超高压榴辉岩(峰期变质230Ma)密切共生, 但是这些花岗质脉体并不具有埃达克岩特征(Wang等, 2014). 可见, 与榴辉岩共生花岗质岩石的形成时代基本都晚于榴辉岩峰期变质作用时代, 其成分除了具有埃达克岩的成分特征外, 也存在不具有埃达克岩成分特征的. 另外, 有研究报道了一些区域(如新西兰、科西斯坦和苏格兰)与麻粒岩相(P=1.0~1.4GPa, T=750~850℃或大于900℃)石榴石角闪岩、石榴石辉石岩共生的花岗质岩石具有高的Sr/Y和Sr值、低Y和Yb含量以及正Sr、Eu异常, 类似于TTG或埃达克岩(例如, Stevenson等, 2005; Garrido等, 2006; Stowell等, 2010; Johnson等, 2012). 因此, 存在的问题包括: (1) 在大于>80km的地幔深度, 沿着俯冲或折返路径, 矿物溶解和元素分配如何变化(Zheng和Hermann, 2014)? (2) 高压-超高压岩石在榴辉岩相峰期变质作用过程中是否能够产生埃达克质熔体? (3) 高压-超高压岩石(榴辉岩及其伴生的中酸性变质岩)在折返过程中产生熔体(包括埃达克质熔体)的温压、含水流体条件及熔体组成是怎样的? (4) 麻粒岩相变质作用究竟是否能够产生埃达克质熔体? 如果可以, 那么这些熔体同榴辉岩相条件下产生的熔体成分、温压

条件与源区残留矿物究竟有什么差别?

7.3 俯冲带板片熔体-地幔相互作用过程与机制

除了板片释放的含水流体之外, 俯冲带熔体-地幔相互作用对弧岩浆源区的形成具有非常重要的作用. 在俯冲带, 通过俯冲作用进入到地幔深处的物质可能包含俯冲玄武质洋壳、陆壳、俯冲板片沉积物、混杂岩、被侵蚀的俯冲上盘物质等, 这些都可能成为埃达克岩的源区物质. 产生的埃达克质岩浆在穿过地幔的过程中, 会同地幔发生强烈的相互作用: 一方面, 地幔的物质进入到岩浆中, 改变岩浆的组成; 另外一方面, 岩浆对地幔进行交代. 熔体与橄榄岩的比例对熔体-地幔相互作用的影响非常大(徐义刚等, 2020). 如果熔体比例小, 只会交代少量橄榄岩; 如果熔体比例大, 除了发生地幔交代作用, 反应后的残余熔体喷出地表会形成岛弧岩石(Rapp等, 1999; 徐义刚等, 2020). 地幔楔内部低熔体/地幔橄榄岩比交代反应可形成岛弧高镁安山岩, 而高熔体/地幔橄榄岩比交代反应则形成岛弧高硅富镁埃达克岩(Su等, 2019). 被熔体交代的地幔发生熔融可以形成富Nb玄武岩、高镁安山岩等(如Sajona等, 1993, 1996; Kepezhinskas等, 1997; Defant和Kepezhinskas, 2001; Defant等, 2002; Bourdon等, 2003). 另外, 板片来源的俯冲组分在一定的深部可能是超临界流体(Kessel等, 2005; Kawamoto等, 2012; Mibe等, 2011; Zheng等, 2011; Ni等, 2017), 并且超临界流体不易保存, 在弧下地幔上升的过程中, 降压会导致其再次分解成富水流体和含水硅酸盐熔体(Kawamoto等, 2012). 因此, 俯冲带中通过俯冲作用进入地幔深部的物质非常复杂, 这些物质除了与地幔混合之外, 还产生熔体、含水流体甚至超临界流体并与地幔发生强烈相互作用, 控制着弧岩浆源区的形成, 影响全球物质的循环(Zheng, 2019). 但是, 这些熔体、含水流体甚至超临界流体如何分别与地幔作用形成不同成分的交代产物以及如何在俯冲带岩浆岩的形成中发挥作用仍然是尚未解决的重要基础科学问题(Zheng和Hermann, 2014).

7.4 太古宙埃达克质TTG的形成与地壳生长、板块构造启动的关联

TTG作为太古宙的大陆地壳最主要的岩石类型, 其形成与板块构造过程、氧气的产生以及地球宜居性演化是否存在关联一直是地球科学的热点问题之一. Defant和Drummond(1990)在提出埃达克岩的概念时就指出, 新生代埃达克岩与太古宙TTG具有类似的成分, 并认为TTG的形成与大洋板块的俯冲、熔融有关. 后来, 许多研究者将二者对比用于揭示太古宙的大陆地壳生长机制、探讨板块构造的启动时间(Martin, 1999; Martin等, 2005; Smithies, 2000; Condie, 2005; Rapp等, 2010; Hastie等, 2010, 2015). 尽管太古宙TTG岩石与埃达克岩有类似的组分, 但其并不具有固定的组分, 而是随着时间变化具有成分上的变化. 例如, >3.5Ga的TTG普遍低Mg、Cr、Ni等, 同时Sr含量也相对低; 而<3.0Ga的TTG具有相对高的Mg、Cr、Ni和Sr含量(Smithies等, 2003; Martin等, 2005). 这样两种情况被认为都与大洋岩石圈的俯冲有关, 前者被认为缺乏地幔楔组分, 后者被认为包含地幔楔组分, 也就是说板块构造过程在>3.5Ga已经启动(Martin, 1999; Martin等, 2005; Hastie等, 2010, 2015). 但是一些研究者坚持, 只有在晚太古宙(3.0~2.5Ga)出现了类似现代弧环境的玻安岩-高镁安山岩(赞岐岩)-富Nb玄武岩-埃达克岩等组合, 类似现代板块构造(大洋俯冲)活动才开始启动(Kerrich等, 1998; Smithies, 2000; Polat等, 2002; Polat和Kerrich, 2002; Smithies等, 2004). 尽管新生代埃达克岩与太古宙TTG的对比研究在揭示太古宙的大陆地壳生长机制、探讨板块构造的启动时间取得了重要进展, 但是许多核心的分歧仍旧存在. 特别是, 从岩浆岩岩石学上得出的结论与构造、沉积、高压-超高压变质以及数值模拟的结果并不一致, 仍旧需要更多深入的研究工作. 因此, 太古宙埃达克质TTG的形成与地壳生长、板块构造启动仍旧是当前国际地质尚未解决的一个热点问题.

7.5 埃达克岩的金属成矿机理

关于埃达克岩与成矿的关系, 一直是研究的热点. 前面已经提到, 埃达克岩为什么易成矿, 影响因素包括俯冲洋壳熔体高氧逸度、岩浆源区(或洋壳)富亲铜元素、埃达克质岩浆富水、岩浆高压分离结晶、增厚的大陆下地壳中角闪石高压下分解、熔体-地幔作用等. 尽管影响因素很多, 但究竟哪一种因素起决定性作用, 二者的本质联系是什么, 依然没有定论. 比如, 一些研究认为富水是埃达克岩形成并伴随金属成矿的重要控制因素(例如, Richards和Kerrich, 2007; Richards, 2011;

Loucks, 2014; Williamson等, 2016; Sillitoe, 2018). 但是, 对日本西南部弧断面的研究观察到了岩浆水含量与岩浆Sr/Y比值呈现负相关, 即高压下相对贫水的岩浆更容易产生埃达克质熔体(Zellmer等, 2012). 最近的研究也发现, 与岩浆热液矿床共生的埃达克岩的形成是从原始贫水、高Sr岩浆体系向富水、低Sr岩浆体系演化的(Zhou等, 2020a). 尽管有研究认为高压条件下石榴石的分离结晶导致的高氧逸度有利于成矿(Lee和Tang, 2020), 但也有研究者认为厚地壳时有更多钙碱性岩浆和铜矿的原因是磁铁矿效应, 即厚地壳岩浆更富水, 结晶磁铁矿导致岩浆含铜硫化物分异, 堆积在下地壳, 后面再成矿(Chiaradia, 2014). Zheng等(2019a)指出, 大洋俯冲增生造山带成矿元素发生富集直至成矿至少可以分为三阶段: (1) 初始富集, 俯冲板片交代地幔楔, 形成富集地幔源区; (2) 二次富集, 地幔楔部分熔融形成富含成矿元素的镁铁质岩浆; (3) 三次富集, 镁铁质岩石在地壳深部部分熔融和结晶分异, 形成与成矿密切相关的长英质斑岩. 按照传统观点, 具有挤压性质的碰撞造山带并不利于形成岩浆-热液型矿床, 但在一些典型的碰撞造山带内, 例如中国青藏高原和秦岭-大别地区, 同样发现有大量的热液矿床(例如, Hou等, 2009; Hou, 2010; Zheng Y F等, 2019). 因此, 大陆碰撞背景下的成矿深部动力学过程是现今矿床学研究的热点和重点之一. 有观点认为, 该背景下的成矿母岩浆是来自早期俯冲阶段堆晶的富金属物质重熔形成(Hou等, 2015; Zheng Y C等, 2019). 也有观点认为, 碰撞造山带中的热液矿床是岩石圈地幔熔融的产物(Lu等, 2015; Holwell等, 2019; Zheng Y F等, 2019), 这些岩石圈地幔在早期大洋俯冲阶段通过交代作用对成矿元素进行了预富集(Zheng Y F等, 2019). 尽管这些认识存在一定的差异性, 但均强调了碰撞造山带内成矿物质的起源与早期大洋俯冲过程具有密切的成因联系(Hou等, 2015; Zheng Y F等, 2019). 此外, 埃达克质岩浆的成矿条件(熔融或流体包裹体成分及产生的温压、水、氧逸度)、不同构造背景中埃达克岩的金属成矿机制、含矿与贫矿埃达克岩的差异及其控制因素等也需要深入研究.

综上分析, 本文提出未来需要研究的领域包括: 不同类型岩石(包括中酸性岩浆岩)在不同温压条件下熔融和分离结晶过程的实验模拟与埃达克质岩浆的产生、岩浆储库演化与埃达克岩的形成、埃达克岩构造背景与成因及动力学过程、板片熔体与地幔相互作用及交代作用、太古宙埃达克质TTG的形成与板块构造启动及地壳生长、不同构造背景中埃达克岩的形成与金属成矿等.

8 结语

埃达克质岩是一类具有特殊地球化学特征和重要地球动力学、成矿意义的中酸性岩浆岩. 新生代俯冲洋壳熔融形成的埃达克岩主要出现于环太平洋火山弧区(洋内弧、大陆弧、陆缘岛弧), 而新生代加厚下地壳部分熔融形成埃达克岩主要出现在特提斯-青藏高原碰撞带. 俯冲洋壳熔融产生的埃达克质岩浆与地幔楔橄榄岩相互作用形成一套特殊的岩石组合——埃达克岩-埃达克型高镁安山岩-Piip型高镁安山岩-富Nb玄武岩-玻安山岩等. 埃达克质岩浆产生的条件为压力1.2~3.0GPa, 温度为800~1000℃, H_2O含量为1.5~6.0wt.%, 源区残留矿物组合为石榴石+金红石, 很少或无斜长石. 一些新生代铜金等矿床的成矿母岩就是埃达克质岩, 暗示埃达克岩具有重要的铜金成矿指示意义及勘探价值. 埃达克岩的研究仍然在一些领域存在薄弱点, 未来埃达克岩的成因及其成矿的研究仍然是一个深入研究的前沿领域.

致谢 感谢主编郑永飞院士邀请撰写本文. 感谢郑永飞院士、马昌前教授、宋述光教授和另外三位匿名审稿人的建议.

参考文献

葛小月, 李献华, 陈志刚, 李伍平. 2002. 中国东部燕山期高Sr低Y型中酸性火成岩的地球化学特征及成因: 对中国东部地壳厚度的制约. 科学通报, 47: 474–480

孙卫东, 凌明星, 杨晓勇, 范蔚茗, 丁兴, 梁华英. 2010. 洋脊俯冲与斑岩铜金矿成矿. 中国科学: 地球科学, 40: 127–137

唐功建, 王强. 2010. 高镁安山岩及其地球动力学意义. 岩石学报, 26: 2495–2512

王强, 赵振华, 熊小林, 许继锋. 2001a. 底侵玄武质下地壳的熔融: 来自安徽沙溪adakite质富钠石英闪长玢岩的证据. 地球化学, 30: 353–362

王强, 许继锋, 赵振华, 王人镜, 邱家骧, 包志伟. 2001b. 大别山燕山期亏损重稀土元素花岗岩类的成因及动力学意义. 岩石学报, 17: 551–564

王强, 唐功建, 郝露露, Wyman D, 马林, 但卫, 张修政, 刘金恒, 黄彤宇, 许传兵. 2020. 洋中脊或海岭俯冲与岩浆作用及金属成矿. 中国科学: 地球科学, 50: 1401–1423

王强, 唐功建, 贾小辉, 资锋, 姜子琦, 许继峰, 赵振华. 2008. 埃达克质岩的金属成矿作用. 高校地质学报, 14: 350–364

王强, 许继峰, 赵振华, 资锋, 唐功建, 贾小辉, 姜子琦. 2007. 中国埃达克岩或埃达克质岩及相关金属成矿作用. 矿物岩石地球化学通报, 26: 336–349

王强, 许继峰, 赵振华. 2003. 强烈亏损重稀土元素中酸性侵入岩(或埃达克质岩)与成矿——以中国东部、青藏高原、新疆北部为例. 地学前缘, 1: 561–572

王强, 赵振华, 许继峰, 李献华, 熊小林, 包志伟, 刘义茂. 2002. 扬子地块东部燕山期埃达克质(adakite-like)岩与成矿. 中国科学D辑: 地球科学, 32(增刊): 127–136

魏春景, 关晓, 董杰. 2017. 基性岩高温-超高温变质作用与TTG质岩成因. 岩石学报, 33: 1381–1404

熊伯琴, 许文良, 李秋立, 杨德彬, 周群君. 2015. 徐淮地区早白垩世Adakitic岩石中榴辉岩类捕虏体中金红石的SIMS U-Pb定年: 对华北克拉通东部陆壳加厚时间的制约. 中国科学: 地球科学, 45: 553–560

熊小林, 刘星成, 朱志敏, 李元, 肖万生, 宋茂双, 张生, 吴金花. 2011. 华北埃达克质岩与克拉通破坏: 实验岩石学和地球化学依据. 中国科学: 地球科学, 41: 654–667

徐义刚, 王强, 唐功建, 王军, 李洪颜, 周金胜, 李奇维, 齐玥, 刘平平, 马林, 范晶晶. 2020. 弧玄武岩的成因: 进展与问题. 中国科学: 地球科学, 50: 1818–1844

詹美珍, 孙卫东, 凌明星, 李贺. 2015. 黄岩海山链俯冲与吕宋岛斑岩铜金成矿. 岩石学报, 31: 2101–2114

张旗, 王焰, 钱青, 杨进辉, 王元龙, 赵太平, 郭光军. 2001. 中国东部中生代埃达克岩的特征及其构造-成矿意义. 岩石学报, 17: 236–244

郑永飞, 陈仁旭, 徐峥, 张少兵. 2016. 俯冲带中的水迁移. 中国科学: 地球科学, 46: 253–286

Abratis M, Wörner G. 2001. Ridge collision, slab-window formation, and the flux of Pacific asthenosphere into the Caribbean realm. Geology, 29: 127–130

Arth J G, Hanson G N. 1972. Quartz diorites derived by partial melting of eclogite or amphibolite at mantle depths. Contrib Mineral Petrol, 37: 161–174

Arth J G, Hanson G N. 1975. Geochemistry and origin of the early Precambrian crust of northeastern Minnesota. Geochim Cosmochim Acta, 39: 325–362

Atherton M P, Petford N. 1993. Generation of sodium-rich magmas from newly underplated basaltic crust. Nature, 362: 144–146

Audétat A, Simon A C. 2012. Magmatic controls on porphyry copper genesis. In: Hedenquist J W, Harris M, Camus F, eds. Geology and Genesis of Major Copper Deposits and Districts of the world: A Tribute to Richard H. Sillitoe. Soc Econom Geol Spec Publ, 16: 553–572

Bachmann O, Huber C. 2016. Silicic magma reservoirs in the Earth's crust. Am Miner, 101: 2377–2404

Baker M B, Hirschmann M M, Ghiorso M S, Stolper E M. 1995. Compositions of near-solidus peridotite melts from experiments and thermodynamic calculations. Nature, 375: 308–311

Baker M B, Stolper E M. 1994. Determining the composition of high-pressure mantle melts using diamond aggregates. Geochim Cosmochim Acta, 58: 2811–2827

Beard B L, Fraracci K N, Clayton R A, Mayeda T K, Snyder G A, Sobolev N V, Taylor L A. 1996. Petrography and geochemistry of eclogites from the Mir kimberlite, Yakutia, Russia. Contrib Mineral Petrol, 125: 293–310

Beate B, Monzier M, Spikings R, Cotten J, Silva J, Bourdon E, Eissen J P. 2001. Mio-Pliocene adakite generation related to flat subduction in southern Ecuador: The Quimsacocha volcanic center. Earth Planet Sci Lett, 192: 561–570

Benoit M, Aguillón-Robles A, Calmus T, Maury R C, Bellon H, Cotten J, Bourgois J, Michaud F. 2002. Geochemical diversity of Late Miocene volcanism in southern Baja California, Mexico: Implication of mantle and crustal sources during the opening of an asthenospheric window. J Geol, 110: 627–648

Bourdon E, Eissen J P, Gutscher M A, Monzier M, Hall M L, Cotten J. 2003. Magmatic response to early aseismic ridge subduction: The Ecuadorian margin case (South America). Earth Planet Sci Lett, 205: 123–138

Bourdon E, Eissen J, Monzier M, Robin C, Martin H, Cotten J, Hall M L. 2002. Adakite-like Lavas from Antisana Volcano (Ecuador): Evidence for Slab Melt Metasomatism Beneath Andean Northern Volcanic Zone. J Petrol, 43: 199–217

Bourgois J, Lagabrielle Y, Martin H, Dyment J, Frutos J, Cisternas M E. 2016. A review on Forearc ophiolite obduction, adakite-like generation, and slab window development at the Chile Triple Junction area: Uniformitarian framework for spreading-ridge subduction. Pure Appl Geophys, 173: 3217–3246

Breitfeld H T, Macpherson C, Hall R, Thirlwall M, Ottley C J, Hennig-Breitfeld J. 2019. Adakites without a slab: Remelting of hydrous basalt in the crust and shallow mantle of Borneo to produce the Miocene Sintang Suite and Bau Suite magmatism of West Sarawak. Lithos, 344-345: 100–121

Breitsprecher K, Thorkelson D J. 2009. Neogene kinematic history of Nazca-Antarctic-Phoenix slab windows beneath Patagonia and the Antarctic Peninsula. Tectonophysics, 464: 10–20

Cameron W E, Nisbet E G, Dietrich V J. 1979. Boninites, komatiites

and ophiolitic basalts. Nature, 280: 550–553
Cashman K V, Giordano G. 2014. Calderas and magma reservoirs. J Volcanol Geotherm Res, 288: 28–45
Castillo P R. 2006. An overview of adakite petrogenesis. Chin Sci Bull, 51: 257–268
Castillo P R. 2012. Adakite petrogenesis. Lithos, 134-135: 304–316
Castillo P R. 2008. Origin of the adakite-high-Nb basalt association and its implications for postsubduction magmatism in Baja California, Mexico. Geol Soc Am Bull, 120: 451–462
Castillo P R, Janney P E, Solidum R U. 1999. Petrology and geochemistry of Camiguin island, southern Philippines: Insights to the source of adakites and other lavas in a complex arc setting. Contrib Mineral Petrol, 134: 33–51
Castillo P R, Rigby S J, Solidum R U. 2007. Origin of high field strength element enrichment in volcanic arcs: Geochemical evidence from the Sulu Arc, southern Philippines. Lithos, 97: 271–288
Chen D L, Liu L, Sun Y, Sun W D, Zhu X H, Liu X M, Guo C L. 2012. Felsic veins within UHP eclogite at xitieshan in north qaidam, NW China: Partial melting during exhumation. Lithos, 136-139: 187–200
Chiaradia M. 2009. Adakite-like magmas from fractional crystallization and melting-assimilation of mafic lower crust (Eocene Macuchi arc, Western Cordillera, Ecuador). Chem Geol, 265: 468–487
Chiaradia M. 2014. Copper enrichment in arc magmas controlled by overriding plate thickness. Nat Geosci, 7: 43–46
Chiaradia M, Caricchi L. 2017. Stochastic modelling of deep magmatic controls on porphyry copper deposit endowment. Sci Rep, 7: 44523
Chung S L, Chu M F, Ji J, O'Reilly S Y, Pearson N J, Liu D, Lee T Y, Lo C H. 2009. The nature and timing of crustal thickening in southern Tibet: Geochemical and zircon Hf isotopic constraints from postcollisional adakites. Tectonophysics, 477: 36–48
Chung S L, Liu D, Ji J, Chu M F, Lee H Y, Wen D J, Lo C H, Lee T Y, Qian Q, Zhang Q. 2003. Adakites from continental collision zones: Melting of thickened lower crust beneath southern Tibet. Geology, 31: 1021–1024
Chung S L, Chu M F, Zhang Y, Xie Y, Lo C H, Lee T Y, Lan C Y, Li X, Zhang Q, Wang Y. 2005. Tibetan tectonic evolution inferred from spatial and temporal variations in post-collisional magmatism. Earth-Sci Rev, 68: 173–196
Coldwell B, Adam J, Rushmer T, MacPherson C G. 2011. Evolution of the East Philippine Arc: Experimental constraints on magmatic phase relations and adakitic melt formation. Contrib Mineral Petrol, 162: 835–848
Cole R B, Stewart B W. 2009. Continental margin volcanism at sites of spreading ridge subduction: Examples from southern Alaska and western California. Tectonophysics, 464: 118–136
Condie K C. 1981. Archean Greenstone Belts. Amsterdam: Elsevier. 434
Condie K C. 2005. High field strength element ratios in Archean basalts: A window to evolving sources of mantle plumes? Lithos, 79: 491–504
Conrey R M, Hooper P R, Larson P B, Chesley J, Ruiz J. 2001. Trace element and isotopic evidence for two types of crustal melting beneath a high Cascade volcanic center, Mt. Jefferson, Oregon. Contrib Mineral Petrol, 141: 710–732
Dai H K, Zheng J, Zhou X, Griffin W L. 2017. Generation of continental adakitic rocks: Crystallization modeling with variable bulk partition coefficients. Lithos, 272-273: 222–231
Danyushevsky L V, Falloon T J, Crawford A J, Tetroeva S A, Leslie R L, Verbeeten A. 2008. High-Mg adakites from Kadavu Island Group, Fiji, southwest Pacific: Evidence for the mantle origin of adakite parental melts. Geology, 36: 499–502
Defant M J, Drummond M S. 1990. Derivation of some modern arc magmas by melting of young subducted lithosphere. Nature, 347: 662–665
Defant M J, Jackson T E, Drummond M S, de Boer J Z, Bellon H, Feigenson M D, Maury R C, Stewart R H. 1992. The geochemistry of young volcanism throughout Western Panama and Southeastern Costa Rica: An overview. J Geol Soc, 149: 569–579
Defant M J, Kepezhinskas P. 2001. Evidence suggests slab melting in arc magmas. Eos Trans AGU, 82: 65–68
Defant M J, Richerson P M, de Boer J Z, Stewart R H, Maury R C, Bellon H, Drummond M S, Feigenson M D, Jackson T E. 1991. Dacite genesis via both slab melting and differentiation: Petrogenesis of La Yeguada Volcanic Complex, Panama. J Petrol, 32: 1101–1142
Defant M J, Xu J F, Kepezhinskas P, Wang Q, Zhang Q, Xiao L. 2002. Adakites: Some variations on a theme. Acta Petrol Sin, 18: 129–142
Dokuz A, Uysal İ, Siebel W, Turan M, Duncan R, Akçay M. 2013. Post-collisional adakitic volcanism in the eastern part of the Sakarya Zone, Turkey: Evidence for slab and crustal melting. Contrib Mineral Petrol, 166: 1443–1468
Drummond M S, Defant M J. 1990. A model for Trondhjemite-Tonalite-Dacite Genesis and crustal growth via slab melting: Archean to modern comparisons. J Geophys Res, 95: 21503–21521
Edmonds M, Cashman K V, Holness M, Jackson M. 2019. Architecture and dynamics of magma reservoirs. Phil Trans R Soc A, 377: 20180298
Falloon T J, Danyushevsky L V, Crawford A J, Meffre S, Woodhead J D, Bloomer S H. 2008. Boninites and adakites from the Northern Termination of the Tonga Trench: Implications for adakite

petrogenesis. J Petrol, 49: 697–715
Ferrero S, Wunder B, Walczak K, O'Brien P J, Ziemann M A. 2015. Preserved near ultrahigh-pressure melt from continental crust subducted to mantle depths. Geology, 43: 447–450
Franz G, Smelik E A. 1995. Zoisite-clinozoisite bearing pegmatites and their importance for decompressional melting in eclogites. Eur J Mineral, 7: 1421–1436
Frisch W, Meschede M, Blakey R. 2011. Plate Tectonics: Continental Drift and Mountain Building. Berlin, Heidelberg: Springer. 212
Gao S, Rudnick R L, Yuan H L, Liu X M, Liu Y S, Xu W L, Ling W L, Ayers J, Wang X C, Wang Q H. 2004. Recycling lower continental crust in the North China craton. Nature, 432: 892–897
Gao X Y, Zheng Y F, Chen Y X, Hu Z. 2013. Trace element composition of continentally subducted slab-derived melt: Insight from multiphase solid inclusions in ultrahigh-pressure eclogite in the Dabie orogen. J Metamorph Geol, 31: 453–468
Gao X Y, Zheng Y F, Chen Y X. 2012. Dehydration melting of ultrahigh-pressure eclogite in the Dabie orogen: Evidence from multiphase solid inclusions in garnet. J Metamorph Geol, 30: 193–212
Gao Y, Hou Z, Kamber B S, Wei R, Meng X, Zhao R. 2007. Adakite-like porphyries from the southern Tibetan continental collision zones: Evidence for slab melt metasomatism. Contrib Mineral Petrol, 153: 105–120
Garrido C J, Bodinier J L, Burg J P, Zeilinger G, Hussain S S, Dawood H, Chaudhry M N, Gervilla F. 2006. Petrogenesis of mafic garnet granulite in the lower crust of the Kohistan paleo-arc complex (Northern Pakistan): Implications for intra-crustal differentiation of island arcs and generation of continental crust. J Petrol, 47: 1873–1914
Gazel E, Hayes J L, Hoernle K, Kelemen P, Everson E, Holbrook W S, Hauff F, van den Bogaard P, Vance E A, Chu S, Calvert A J, Carr M J, Yogodzinski G M. 2015. Continental crust generated in oceanic arcs. Nat Geosci, 8: 321–327
Ge R, Zhu W, Wilde S A, Wu H. 2018. Remnants of eoarchean continental crust derived from a subducted proto-arc. Sci Adv, 4: eaao3159
Gill J B. 1981. Orogenic Andesite and Plate Tectonics. Berlin: Springer
Goss A R, Kay S M. 2006. Steep REE patterns and enriched Pb isotopes in southern Central American arc magmas: Evidence for forearc subduction erosion? Geochem Geophys Geosyst, 7: Q05016
Goss A R, Kay S M, Mpodozis C. 2013. Andean adakite-like high-Mg andesites on the northern margin of the Chilean-Pampean Flat-slab (27–28.5°S) associated with frontal arc migration and fore-arc subduction erosion. J Petrol, 54: 2193–2234
Green T H, Ringwood A E. 1968. Genesis of the calc-alkaline igneous rock suite. Contrib Mineral Petrol, 18: 105–162
Gromet P, Silver L T. 1987. REE variations across the peninsular ranges batholith: Implications for batholithic petrogenesis and crustal growth in magmatic arcs. J Petrol, 28: 75–125
Guo F, Nakamuru E, Fan W M, Kobayoshi K, Li C W. 2007. Generation of Palaeocene adakitic andesites by magma mixing; Yanji Area, NE China. J Petrol, 48: 661–692
Guo Z, Wilson M, Liu J. 2007. Post-collisional adakites in south Tibet: Products of partial melting of subduction-modified lower crust. Lithos, 96: 205–224
Gutscher M A, Maury R, Eissen J P, Bourdon E. 2000. Can slab melting be caused by flat subduction? Geology, 28: 535–538
Harris N R, Sisson V B, Wright J E, Pavlis T L. 1996. Evidence for Eocene mafic underplating during fore-arc intrusive activity, eastern Chugach Mountains, Alaska. Geology, 24: 263–264
Hastie A R, Fitton J G, Mitchell S F, Neill I, Nowell G M, Millar I L. 2015. Can fractional crystallization, mixing and assimilation processes be responsible for Jamaican-type adakites? Implications for generating Eoarchaean continental crust. J Petrol, 56: 1251–1284
Hastie A R, Kerr A C, McDonald I, Mitchell S F, Pearce J A, Wolstencroft M, Millar I L. 2010. Do Cenozoic analogues support a plate tectonic origin for Earth's earliest continental crust? Geology, 38: 495–498
Hao L L, Wang Q, Zhang C, Ou Q, Yang J H, Dan W, Jiang Z Q. 2019. Oceanic plateau subduction during closure of the Bangong-Nujiang Tethyan Ocean: Insights from central Tibetan volcanic rocks. Geol Soc Am Bull, 131: 864–880
He Y S, Wu H, Ke S, Liu S A, Wang Q. 2017. Iron isotopic compositions of adakitic and non-adakitic granitic magmas: Magma compositional control and subtle residual garnet effect. Geochim Cosmochim Acta, 203: 89–102
He Y, Li S G, Hoefs J, Huang F, Liu S A, Hou Z. 2011. Post-collisional granitoids from the Dabie orogen: New evidence for partial melting of a thickened continental crust. Geochim Cosmochim Acta, 75: 3815–3838
Hernández-Uribe D, Hernández-Montenegro J D, Cone K A, Palin R M. 2020. Oceanic slab-top melting during subduction: Implications for trace-element recycling and adakite petrogenesis. Geology, 48: 216–220
Hedenquist J W, Lowenstern J B. 1994. The role of magmas in the formation of hydrothermal ore deposits. Nature, 370: 519–527
Hermann J, Zheng Y F, Rubatto D. 2013. Deep fluids in subducted continental crust. Elements, 9: 281–287
Hirose K. 1997. Melting experiments on lherzolite KLB-1 under hydrous conditions and generation of high-magnesian andesitic melts. Geology, 25: 42–44
Hirose K, Kawamoto T. 1995. Hydrous partial melting of lherzolite at 1 GPa: The effect of H_2O on the genesis of basaltic magmas. Earth

Planet Sci Lett, 133: 463–473

Hirose K, Kushiro I. 1993. Partial melting of dry peridotites at high pressures: Determination of compositions of melts segregated from peridotite using aggregates of diamond. Earth Planet Sci Lett, 114: 477–489

Hirose K, Kushiro I. 1998. The effect of melt segregation on polybaric mantle melting: Estimation from the incremental melting experiments. Phys Earth Planet Inter, 107: 111–118

Holwell D A, Fiorentini M, McDonald I, Lu Y, Giuliani A, Smith D J, Keith M, Locmelis M. 2019. A metasomatized lithospheric mantle control on the metallogenic signature of post-subduction magmatism. Nat Commun, 10: 1

Horodyskyj U N, Lee C T A, Ducea M N. 2007. Similarities between Archean high MgO eclogites and Phanerozoic arc-eclogite cumulates and the role of arcs in Archean continent formation. Earth Planet Sci Lett, 256: 510–520

Hou Z Q. 2010. Metallogensis of continental collision. Acta Petrol Sin, 84: 30–58

Hou Z, Cook N J. 2009. Metallogenesis of the Tibetan collisional orogen: A review and introduction to the special issue. Ore Geol Rev, 36: 2–24

Hou Z Q, Gao Y F, Qu X M, Rui Z Y, Mo X X. 2004. Origin of adakitic intrusives generated during mid-Miocene east-west extension in southern Tibet. Earth Planet Sci Lett, 220: 139–155

Hou Z Q, Zheng Y C, Zeng L S, Gao L E, Huang K X, Li W, Li Q Y, Fu Q, Liang W, Sun Q Z. 2012. Eocene-Oligocene granitoids in southern Tibet: Constraints on crustal anatexis and tectonic evolution of the Himalayan orogen. Earth Planet Sci Lett, 349-350: 38–52

Hou Z, Yang Z, Lu Y, Kemp A, Zheng Y, Li Q, Tang J, Yang Z, Duan L. 2015. A genetic linkage between subduction- and collision-related porphyry Cu deposits in continental collision zones. Geology, 43: 247–250

Hou Z, Yang Z, Qu X, Meng X, Li Z, Beaudoin G, Rui Z, Gao Y, Zaw K. 2009. The Miocene Gangdese porphyry copper belt generated during post-collisional extension in the Tibetan Orogen. Ore Geol Rev, 36: 25–51

Hu P, Cao L, Zhang H, Yang Q, Armin T, Cheng X. 2019. Late Miocene adakites associated with the Tangse porphyry Cu-Mo deposit within the Sunda arc, north Sumatra, Indonesia. Ore Geol Rev, 111: 102983

Huang J, Zhang X C, Chen S, Tang L, Wörner G, Yu H, Huang F. 2018. Zinc isotopic systematics of Kamchatka-Aleutian arc magmas controlled by mantle melting. Geochim Cosmochim Acta, 238: 85–101

Ickert R B, Thorkelson D J, Marshall D D, Ullrich T D. 2009. Eocene adakitic volcanism in southern British Columbia: Remelting of arc basalt above a slab window. Tectonophysics, 464: 164–185

Ireland T R, Rudnick R L, Spetsius Z. 1994. Trace elements in diamond inclusions from eclogites reveal link to Archean granites. Earth Planet Sci Lett, 128: 199–213

Ishizuka O, Kimura J I, Li Y B, Stern R J, Reagan M K, Taylor R N, Ohara Y, Bloomer S H, Ishii T, Hargrove U S, Haraguchi S. 2006. Early stages in the evolution of Izu-Bonin arc volcanism: New age, chemical, and isotopic constraints. Earth Planet Sci Lett, 250: 385–401

Ishizuka O, Tani K, Reagan M K, Kanayama K, Umino S, Harigane Y, Sakamoto I, Miyajima Y, Yuasa M, Dunkley D J. 2011. The timescales of subduction initiation and subsequent evolution of an oceanic island arc. Earth Planet Sci Lett, 306: 229–240

Jacob D, Jagoutz E, Lowry D, Mattey D, Kudrjavtseva G. 1995. Diamondiferous eclogites from Siberia: Remnants of Archean oceanic crust. Geochim Cosmochim Acta, 58: 5191–5207

Jahangiri A. 2007. Post-collisional Miocene adakitic volcanism in NW Iran: Geochemical and geodynamic implications. J Asian Earth Sci, 30: 433–447

Jiang N, Liu Y, Zhou W, Yang J, Zhang S. 2007. Derivation of Mesozoic adakitic magmas from ancient lower crust in the North China craton. Geochim Cosmochim Acta, 71: 2591–2608

Jiang Z Q, Wang Q, Wyman D A, Li Z X, Yang J H, Shi X B, Ma L, Tang G J, Gou G N, Jia X H, Guo H F. 2014. Transition from oceanic to continental lithosphere subduction in southern Tibet: Evidence from the Late Cretaceous-Early Oligocene (~91–30 Ma) intrusive rocks in the Chanang-Zedong area, southern Gangdese. Lithos, 196-197: 213–231

Johnson T E, Brown M, Gardiner N J, Kirkland C L, Smithies R H. 2017. Earth's first stable continents did not form by subduction. Nature, 543: 239–242

Johnson T E, Fischer S, White R W, Brown M, Rollinson H R. 2012. Archaean intracrustal differentiation from partial melting of meta-gabbro—Field and geochemical evidence from the central region of the Lewisian Complex, NW Scotland. J Petrol, 53: 2115–2138

Kamei A, Miyake Y, Owada M, Kimura J I. 2009. A pseudo adakite derived from partial melting of tonalitic to granodioritic crust, Kyushu, southwest Japan arc. Lithos, 112: 615–625

Kawamoto T, Kanzaki M, Mibe K, Matsukage K N, Ono S. 2012. Separation of supercritical slab-fluids to form aqueous fluid and melt components in subduction zone magmatism. Proc Natl Acad Sci USA, 109: 18695–18700

Kay R W. 1978. Aleutian magnesian andesites: Melts from subducted Pacific Ocean crust. J Volcanol Geotherm Res, 4: 117–132

Kay R W, Mahlburg S. 1991. Creation and destruction of lower continental crust. Geol Rundsch, 80: 259–278

Kay R W, Mahlburg S. 1993. Delamination and delamination magmatism. Tectonophysics, 219: 177–189

Kay S M, Mpodozis C. 2001. Central Andean ore deposits linked to evolving shallow subduction systems and thickening crust. GSA Today, 11: 4–9

Kay S M, Ramos V A, Marquez M. 1993. Evidence in Cerro Pampa volcanic rocks for slab-melting prior to ridge-trench collision in Southern South America. J Geol, 101: 703–714

Kepezhinskas P K, Defant M J, Drummond M S. 1995. Na metasomatism in the island arc mantle by slab melt-peridotite interaction: Evidence from mantle xenoliths in the North Kamchatka arc. J Petrol, 36: 1505–1527

Kepezhinskas P, McDermott F, Defant M J, Hochstaedter A, Drummond M S, Hawkesworth C J, Koloskov A, Maury R C, Bellon H. 1997. Trace element and Sr-Nd-Pb isotopic constraints on a three-component model of Kamchatka Arc petrogenesis. Geochim Cosmochim Acta, 61: 577–600

Kepezhinskas P, Defant M J. 1996. Contrasting styles of mantle metasomatism above subduction zones: Constraints from ultramafic xenoliths in Kamchatka. In: Bebout G E, Scholl D W, Kirby S H, Platt J P, eds. Subduction: Top to Bottom. AGU Geophys Monogr, 96: 307–314

Kerrich R, Wyman D, Fan J, Bleeker W. 1998. Boninite series: Low Ti-tholeiite associations from the 2.7 Ga Abitibi greenstone belt. Earth Planet Sci Lett, 164: 303–316

Kessel R, Schmidt M W, Ulmer P, Pettke T. 2005. Trace element signature of subduction-zone fluids, melts and supercritical liquids at 120–180 km depth. Nature, 437: 724–727

Kikuchi Y. 1890. On pyorxene components in certain volcanic rocks from Bonin Island. J Coll Sci Imp Univ Jpn, 3: 67–89

König S, Schuth S, Münker C, Qopoto C. 2007. The role of slab melting in the petrogenesis of high-Mg andesites: Evidence from Simbo Volcano, Solomon Islands. Contrib Mineral Petrol, 153: 85–103

Kushiro I. 1996. Partial melting of a fertile mantle peridotite at high pressures: An experimental study using aggregates of diamond. In: Basu A, Hart S R, eds. Earth Processes: Reading the Isotopic Code. Washington DC: American Geophysical Union. 109–122

Le Bas M J. 2000. IUGS reclassification of the high-Mg and picritic volcanic rocks. J Petrol, 41: 1467–1470

Le Bas M J, Le Maitre R W, Streckeisen A, Zanettin B. 1986. A chemical classification of volcanic rocks based on the total alkali-silica diagram. J Petrol, 27: 745–750

Lee C, King S D. 2010. Why are high-Mg# andesites widespread in the western Aleutians? A numerical model approach. Geology, 38: 583–586

Lee C T A, Tang M. 2020. How to make porphyry copper deposits. Earth Planet Sci Lett, 529: 115868

Le Maitre R W. 2002. Igneous Rocks: A Classification and Glossary of Terms. 2nd ed. Cambridge: Cambridge University Press. 1–232

Li J W, Zhao X F, Zhou M F, Ma C Q, de Souza Z S, Vasconcelos P. 2009. Late Mesozoic magmatism from the Daye region, eastern China: U-Pb ages, petrogenesis, and geodynamic implications. Contrib Mineral Petrol, 157: 383–409

Li X H, Li Z X, Li W X, Wang X C, Gao Y. 2013. Revisiting the "C-type adakites" of the Lower Yangtze River Belt, central eastern China: In-situ zircon Hf-O isotope and geochemical constraints. Chem Geol, 345: 1–15

Li Y B, Kimura J I, Machida S, Ishii T, Ishiwatari A, Maruyama S, Qiu H N, Ishikawa T, Kato Y, Haraguchi S, Takahata N, Hirahara Y, Miyazaki T. 2013. High-Mg adakite and low-Ca boninite from a Bonin Fore-arc seamount: Implications for the reaction between slab melts and depleted mantle. J Petrol, 54: 1149–1175

Liebscher A, Franz G, Frei D, Dulski P. 2007. High-pressure melting of eclogite and the *P-T-X* history of tonalitic to trondhjemitic zoisite-pegmatites, Munchberg Massif, Germany. J Petrol, 48: 1001–1019

Ling M X, Wang F Y, Ding X, Hu Y H, Zhou J B, Zartman R E, Yang X Y, Sun W. 2009. Cretaceous ridge subduction along the Lower Yangtze river belt, eastern China. Econ Geol, 104: 303–321

Liu D, Zhao Z, DePaolo D J, Zhu D C, Meng F Y, Shi Q, Wang Q. 2017. Potassic volcanic rocks and adakitic intrusions in southern Tibet: Insights into mantle-crust interaction and mass transfer from Indian plate. Lithos, 268-271: 48–64

Liu S A, Li S, He Y, Huang F. 2010. Geochemical contrasts between early Cretaceous ore-bearing and ore-barren high-Mg adakites in central-eastern China: Implications for petrogenesis and Cu-Au mineralization. Geochim Cosmochim Acta, 74: 7160–7178

Long X, Wilde S A, Wang Q, Yuan C, Wang X C, Li J, Jiang Z, Dan W. 2015. Partial melting of thickened continental crust in central Tibet: Evidence from geochemistry and geochronology of Eocene adakitic rhyolites in the northern Qiangtang Terrane. Earth Planet Sci Lett, 414: 30–44

López-Escobar L, Frey F A, Oyarzun J. 1979. Geochemical characteristics of central Chile (33°–34°S) granitoids. Contrib Mineral Petrol, 70: 439–450

López-Escobar L, Frey F A, Vergara M. 1977. Andesites and high-alumina Basalts from the Central-South Chile high Andes: Geochemical evidence bearing on their petrogenesis. Contrib Mineral Petrol, 63: 199–228

Loucks R R. 2014. Distinctive composition of copper-ore-forming arcmagmas. Australian J Earth Sci, 61: 5–16

Lu Y J, Loucks R R, Fiorentini M L, Yang Z M, Hou Z Q. 2015. Fluid flux melting generated postcollisional high Sr/Y copper ore-forming

water-rich magmas in Tibet. Geology, 43: 583–586

Ma L, Wang B D, Jiang Z Q, Wang Q, Li Z X, Wyman D A, Zhao S R, Yang J H, Gou G N, Guo H F. 2014. Petrogenesis of the Early Eocene adakitic rocks in the Napuri area, southern Lhasa: Partial melting of thickened lower crust during slab break-off and implications for crustal thickening in southern Tibet. Lithos, 196-197: 321–338

Ma Q, Xu Y G, Zheng J P, Sun M, Griffin W L, Wei Y, Ma L, Yu X. 2016. High-Mg adakitic rocks and their complementary cumulates formed by crystal fractionation of hydrous mafic magmas in a continental crustal magma chamber. Lithos, 260: 211–224

Ma Q, Zheng J, Griffin W L, Zhang M, Tang H, Su Y, Ping X. 2012. Triassic “adakitic” rocks in an extensional setting (North China): Melts from the cratonic lower crust. Lithos, 149: 159–173

Ma Q, Zheng J P, Xu Y G, Griffin W L, Zhang R S. 2015. Are continental “adakites” derived from thickened or foundered lower crust? Earth Planet Sci Lett, 419: 125–133

Macpherson C G, Dreher S T, Thirlwall M F. 2006. Adakites without slab melting: High pressure differentiation of island arc magma, Mindanao, the Philippines. Earth Planet Sci Lett, 243: 581–593

Marchev P, Georgiev S, Raicheva R, Peytcheva I, von Quadt A, Ovtcharova M, Bonev N. 2013. Adakitic magmatism in post-collisional setting: An example from the Early-Middle Eocene Magmatic Belt in Southern Bulgaria and Northern Greece. Lithos, 180-181: 159–180

Martin H. 1986. Effect of steeper Archean geothermal gradient on geochemistry of subduction-zone magmas. Geology, 14: 753–756

Martin H. 1999. Adakitic magmas: Modern analogues of Archaean granitoids. Lithos, 46: 411–429

Martin H, Smithies R H, Rapp R, Moyen J F, Champion D. 2005. An overview of adakite, tonalite-trondhjemite-granodiorite (TTG), and sanukitoid: Relationships and some implications for crustal evolution. Lithos, 79: 1–24

Martínez-Serrano R G, Schaaf P, Solís-Pichardo G, Hernández-Bernal M S, Hernández-Treviño T, Julio Morales-Contreras J, Macías J L. 2004. Sr, Nd and Pb isotope and geochemical data from the Quaternary Nevado de Toluca volcano, a source of recent adakitic magmatism, and the Tenango Volcanic Field, Mexico. J Volcanol Geotherm Res, 138: 77–110

Maury R C, Calmus T, Pallares C, Benoit M, Gregoire M, Aguillon-Robles A, Bellon H, Bohn M. 2009. Origin of the adakite-high-Nb basalt association and its implications for postsubduction magmatism in Baja California, Mexico: Discussion. Geol Soc Am Bull, 121: 1465–1469

McGeary S, Nur A, Ben-Avraham Z. 1985. Spatial gaps in arc volcanism: The effect of collision or subduction of oceanic plateaus. Tectonophysics, 119: 195–221

McCarron J J, Smellie J L. 1998. Tectonic implications of fore-arc magmatism and generation of high-magnesian andesites: Alexander Island, Antarctica. J Geol Soc, 155: 269–280

MacGregor I D, Manton W I. 1986. Roberts Victor Eclogites: Ancient oceanic crust. J Geophys Res, 91: 14063–14079

Mibe K, Kawamoto T, Matsukage K N, Fei Y, Ono S. 2011. Slab melting versus slab dehydration in subduction-zone magmatism. Proc Natl Acad Sci USA, 108: 8177–8182

Mints M V, Belousova E A, Konilov A N, Natapov L M, Shchipansky A A, Griffin W L, O’Reilly S Y, Dokukina K A, Kaulina T V. 2010. Mesoarchean subduction processes: 2.87 Ga eclogites from the Kola Peninsula, Russia. Geology, 38: 739–742

Mints M V, Dokukina K A, Konilov A N. 2014. The Meso-Neoarchaean Belomorian eclogite province: Tectonic position and geodynamic evolution. Gondwana Res, 25: 561–584

Moghadam H S, Rossetti F, Lucci F, Chiaradia M, Gerdes A, Martinez M L, Ghorbani G, Nasrabady M. 2016. The calc-alkaline and adakitic volcanism of the Sabzevar structural zone (NE Iran): Implications for the Eocene magmatic flare-up in Central Iran. Lithos, 248-251: 517–535

Morris P A. 1995. Slab melting as an explanation of Quaternary volcanism and aseismicity in southwest Japan. Geology, 23: 395–398

Mungall J E. 2002. Roasting the mantle: Slab melting and the genesis of major Au and Au-rich Cu deposits. Geology, 30: 915–918

Müntener O, Ulmer P. 2006. Experimentally derived high-pressure cumulates from hydrous arc magmas and consequences for the seismic velocity structure of lower arc crust. Geophys Res Lett, 33: L21308

Nair R, Chacko T. 2008. Role of oceanic plateaus in the initiation of subduction and origin of continental crust. Geology, 36: 583–586

Ni H, Zhang L, Xiong X, Mao Z, Wang J. 2017. Supercritical fluids at subduction zones: Evidence, formation condition, and physico-chemical properties. Earth-Sci Rev, 167: 62–71

Nia H M, Baghban S, Simmonds V. 2017. Geology, geochemistry and petrogenesis of post-collisional adakitic intrusions and related dikes in the Khoynarood area, NW Iran. Geochemistry, 77: 53–67

Nicholls I A. 1974. Liquids in equilibrium with peridotitic mineral assemblages at high water pressures. Contrib Mineral Petrol, 45: 289–316

Nisbet E G. 1984. The continental and oceanic crust and lithosphere in the Archaean: Isostatic, thermal, and tectonic models. Can J Earth Sci, 21: 1426–1441

Omrani J, Agard P, Whitechurch H, Benoit M, Prouteau G, Jolivet L. 2008. Arc-magmatism and subduction history beneath the Zagros Mountains, Iran: A new report of adakites and geodynamic

consequences. Lithos, 106: 380–398

Ou Q, Wang Q, Wyman D A, Zhang H X, Yang J H, Zeng J P, Hao L L, Chen Y W, Liang H, Qi Y. 2017. Eocene adakitic porphyries in the central-northern Qiangtang Block, central Tibet: Partial melting of thickened lower crust and implications for initial surface uplifting of the plateau. J Geophys Res-Solid Earth, 122: 1025–1053

Oyarzun R, Márquez A, Lillo J, López I, Rivera S. 2001. Giant versus small porphyry copper deposits of Cenozoic age in northern Chile: Adakitic versus normal calc-alkaline magmatism. Miner Depos, 36: 794–798

Palin R M, White R W, Green E C R. 2016. Partial melting of metabasic rocks and the generation of tonalitic-trondhjemitic-granodioritic (TTG) crust in the archaean: Constraints from phase equilibrium modelling. Precambrian Res, 287: 73–90

Pallares C, Maury R C, Bellon H, Royer J Y, Calmus T, Aguillón-Robles A, Cotten J, Benoit M, Michaud F, Bourgois J. 2007. Slab-tearing following ridge-trench collision: Evidence from Miocene volcanism in Baja California, México. J Volcanol Geotherm Res, 161: 95–117

Pang K N, Chung S L, Zarrinkoub M H, Li X H, Lee H Y, Lin T H, Chiu H Y. 2016. New age and geochemical constraints on the origin of Quaternary adakite-like lavas in the Arabia-Eurasia collision zone. Lithos, 264: 348–359

Payot B D, Jego S, Maury R C, Polve M, Gregoire M, Ceuleneer G, Tamayo Jr R A, Yumul Jr G P, Bellon H, Cotten J. 2007. The oceanic substratum of Northern Luzon: Evidence from xenoliths within Monglo adakite (the Philippines). Island Arc, 16: 276–290

Peacock S M, Rushmer T, Thompson A B. 1994. Partial melting of subducting oceanic crust. Earth Planet Sci Lett, 121: 227–244

Peacock S M, Wang K. 1999. Seismic consequences of warm versus cool subduction metamorphism: Examples from southwest and northeast Japan. Science, 286: 937–939

Peccerillo A, Taylor S R. 1976. Geochemistry of Eocene calc-alkaline volcanic rocks from the Kastamonu area, northern Turkey. Contrib Mineral Petrol, 58: 63–81

Petrone C M, Ferrari L. 2008. Quaternary adakite-Nb-enriched basalt association in the western Trans-Mexican Volcanic Belt: Is there any slab melt evidence? Contrib Mineral Petrol, 156: 73–86

Pineda-Velasco I, Kitagawa H, Nguyen T T, Kobayashi K, Nakamura E. 2018. Production of high-Sr andesite and dacite magmas by melting of subducting oceanic lithosphere at propagating slab tears. J Geophys Res-Solid Earth, 123: 3698–3728

Petford N, Atherton M. 1996. Na-rich partial melts from newly underplated basaltic crust: The Cordillera Blanca Batholith, Peru. J Petrol, 37: 1491–1521

Polat A, Hofmann A W, Rosing M T. 2002. Boninite-like volcanic rocks in the 3.7–3.8 Ga Isua greenstone belt, West Greenland: Geochemical evidence for intra-oceanic subduction zone processes in the early Earth. Chem Geol, 184: 231–254

Polat A, Kerrich R. 2002. Nd-isotope systematics of ~2.7 Ga adakites, magnesian andesites, and arc basalts, Superior Province: Evidence for shallow crustal recycling at Archean subduction zones. Earth Planet Sci Lett, 202: 345–360

Prouteau G, Scaillet B, Pichavant M, Maury R. 2001. Evidence for mantle metasomatism by hydrous silicic melts derived from subducted oceanic crust. Nature, 410: 197–200

Qian Q, Hermann J. 2013. Partial melting of lower crust at 10–15 kbar: Constraints on adakite and TTG formation. Contrib Mineral Petrol, 165: 1195–1224

Rabbia O, Correa K J, Hernandez L B, Ulrich T. 2017. “Normal” to adakite-like arc magmatism associated with the El Abra porphyry copper deposit, Central Andes, Northern Chile. Inter J Earth Sci, 106: 2687–2711

Rapp R P. 1995. Amphibole-out phase boundary in partially melted metabasalt, its control over liquid fraction and composition, and source permeability. J Geophys Res, 100: 15601–15610

Rapp R P, Norman M D, Laporte D, Yaxley G M, Martin H, Foley S F. 2010. Continent formation in the archean and chemical evolution of the cratonic lithosphere: Melt-rock reaction experiments at 3–4 GPa and petrogenesis of Archean Mg-diorites (sanukitoids). J Petrol, 51: 1237–1266

Rapp R P, Shimizu N, Norman M D, Applegate G S. 1999. Reaction between slab-derived melts and peridotite in the mantle wedge: Experimental constraints at 3.8 GPa. Chem Geol, 160: 335–356

Rapp R P, Shimizu N, Norman M D. 2003. Growth of early continental crust by partial melting of eclogite. Nature, 425: 605–609

Rapp R P, Watson E B, Miller C F. 1991. Partial melting of amphibolite/eclogite and the origin of Archean trondhjemites and tonalites. Precambrian Res, 51: 1–25

Rapp R P, Watson E B. 1995. Dehydration melting of metabasalt at 8–32 kbar: Implications for continental growth and crust-mantle recycling. J Petrol, 36: 891–931

Reich M, Parada M A, Palacios C, Dietrich A, Schultz F, Lehmann B. 2003. Adakite-like signature of late miocene intrusions at the los pelambres giant porphyry copper deposit in the andes of central Chile: Metallogenic implications. Mineralium Deposita, 38: 876–885

Richards J P, Kerrich R. 2007. Special paper: Adakite-like rocks: Their diverse origins and questionable role in metallogenesis. Econ Geol, 102: 537–576

Richards J P. 2003. Tectono-magmatic precursors for porphyry Cu-(Mo-Au) deposit formation. Econ Geol, 98: 1515–1533

Richards J P. 2011. High Sr/Y arc magmas and porphyry Cu±Mo±Au deposits: Just add water. Econ Geol, 106: 1075–1081

Ringwood A E. 1974. The petrological evolution of island arc systems. J Geol Soc, 130: 183–204

Rodríguez C, Selles D, Dungan M, Langmuir C, Leeman W. 2007. Adakitic dacites formed by intracrustal crystal fractionation of water-rich parent magmas at Nevado de Longaví volcano (36.2°S; Andean Southern Volcanic Zone, central Chile). J Petrol, 48: 2033–2061

Rogers G, Saunders A D, Terrell D J, Verma S P, Marriner G F. 1985. Geochemistry of Holocene volcanic rocks associated with ridge subduction in Baja California, Mexico. Nature, 315: 389–392

Rollinson H. 1997. Eclogite xenoliths in West African kimberlites as residues from Archaean granitoid crust formation. Nature, 389: 173–176

Rooney T O, Franceschi P, Hall C M. 2011. Water-saturated magmas in the Panama Canal region: A precursor to adakite-like magma generation? Contrib Mineral Petrol, 161: 373–388

Rose E F, Shimizu N, Layne G D, Grove T L. 2001. Melt production beneath Mt. Shasta from boron data in primitive melt inclusions. Science, 293: 281–283

Rosenbaum G, Gasparon M, Lucente F P, Peccerillo A, Miller M S. 2008. Kinematics of slab tear faults during subduction segmentation and implications for Italian magmatism. Tectonics, 27: TC2008

Rudnick R L, Barth M, Horn I, McDonough W F. 2000. Rutile-bearing refractory eclogites: Missing link between continents and depleted mantle. Science, 287: 278–281

Sajona F G, Maury R C, Bellon H, Cotten J, Defant M J, Pubellier M. 1993. Initiation of subduction and the generation of slab melts in Western and Eastern Mindanao, Philippines. Geology, 21: 1007–1010

Sajona F G, Bellon H, Maury R C, Pubellier M, Cotten J, Rangin C. 1994. Magmatic response to abrupt changes in geodynamic settings: Pliocene-Quaternary calc-alkaline and Nb-enriched lavas from Mindanao (Philippines). Tectonophysics, 237: 47–72

Sajona F G, Maury R C, Bellon H, Cotten J, Defant M. 1996. High field strength element enrichment of Pliocene-Pleistocene island arc basalts, Zamboanga Peninsula, Western Mindanao (Philippines). J Petrol, 37: 693–726

Sajona F G, Maury R C. 1998. Association of adakites with gold and copper mineralization in the Philippines. C R Acad Sci II A, 326: 27–34

Samaniego P, Martin H, Robin C, Monzier M. 2002. Transition from calc-alkalic to adakitic magmatism at Cayambe volcano, Ecuador: Insights into slab melts and mantle wedge interactions. Geology, 30: 967–970

Saunders A D, Rogers G, Marriner G F, Terrell D J, Verma S P. 1987. Geochemistry of Cenezoic volcanic rocks, Baja California, Mexico: Implications for the petrogenesis of post-subduction magmas. J Volcanol Geotherm Res, 32: 223–245

Schiano P, Clocchiatti R, Shimizu N, Maury R C, Jochum K P, Hofmann A W. 1995. Hydrous, silica-rich melts in the sub-arc mantle and their relationship with erupted arc lavas. Nature, 377: 595–600

Schmidt M W, Poli S. 2014. Devolatilization during subduction. Treatise on Geochemistry, 4: 669–701

Schuth S, Münker C, König S, Qopoto C, Basi S, Garbe-Schönberg D, Ballhaus C. 2009. Petrogenesis of lavas along the solomon island arc, sw pacific: Coupling of compositional variations and subduction zone geometry. J Petrol, 50: 781–811

Seghedi I, Downes H, Szakacs A, Mason P R, Thirlwall M F, Rosu E, Pecskay Z, Marton E, Panaiotu C. 2004. Neogene-Quaternary magmatism and geodynamics in the Carpathian-Pannonian region: A synthesis. Lithos, 72: 117–146

Sen C, Dunn T. 1994. Dehydration melting of a basaltic composition amphibolite at 1.5 and 2.0 GPa: Implications for the origin of adakites. Contrib Mineral Petrol, 117: 394–409

Sheppard S, Griffin T J, Tyler I M, Page R W. 2001. High- and Low-K granites and adakites at a Palaeoproterozoic plate boundary in northwestern Australia. J Geol Soc, 158: 547–560

Sillitoe R H. 2010. Porphyry copper systems. Econ Geol, 105: 3–41

Sillitoe R H. 2018. Why no porphyry copper deposits in Japan and South Korea? Resour Geol, 68: 107–125

Sisson T W, Kelemen P B. 2018. Near-solidus melts of MORB + 4 wt.% H_2O at 0.8–2.8 GPa applied to issues of subduction magmatism and continent formation. Contrib Mineral Petrol, 173: 70

Skjerlie K P, Patiño Douce A E. 2002. The Fluid-absent Partial Melting of a Zoisite-bearing Quartz Eclogite from 1.0 to 3.2 GPa; Implications for Melting in Thickened Continental Crust and for Subduction-zone Processes. J Petrol, 43: 291–314

Smithies R H, Champion D C, Cassidy K F. 2003. Formation of Earth's early Archaean continental crust. Precambrian Res, 127: 89–101

Smithies R H. 2000. The Archaean tonalite-trondhjemite-granodiorite (TTG) series is not an analogue of Cenozoic adakite. Earth Planet Sci Lett, 182: 115–125

Smithies R H, Champion D C, Sun S S. 2004. Evidence for early LREE-enriched mantle source regions: Diverse magmas from the c. 3.0 Ga Mallina Basin, Pilbara Craton, NW Australia. J Petrol, 45: 1515–1537

Snyder G A, Taylor L A, Crozaz G, Halliday A N, Beard B L, Sobolev V N, Sobolev N V. 1997. The origins of Yakutian eclogite xenoliths. J Petrol, 38: 85–113

Song S, Niu Y, Su L, Wei C, Zhang L. 2014. Adakitic (tonalitic-trondhjemitic) magmas resulting from eclogite decompression and dehydration melting during exhumation in response to continental collision. Geochim Cosmochim Acta, 130: 42–62

Sparks R S J, Annen C, Blundy J D, Cashman K V, Rust A C, Jackson M D. 2019. Formation and dynamics of magma reservoirs. Phil Trans R Soc A, 377: 20180019

Stern C R, Kilian R. 1996. Role of the subducted slab, mantle wedge and continental crust in the generation of adakites from the Andean Austral Volcanic Zone. Contrib Mineral Petrol, 123: 263–281

Stevenson J A, Daczko N R, Clarke G L, Pearson N, Klepeis K A. 2005. Direct observation of adakite melts generated in the lower continental crust, Fiordland, New Zealand. Terra Nova, 17: 73–79

Stöckhert B, Duyster J, Trepmann C, Massonne H J. 2001. Microdiamond daughter crystals precipitated from supercritical COH+silicate fluids included in garnet, Erzgebirge, Germany. Geology, 29: 391–394

Stowell H, Tulloch A, Zuluaga C, Koenig A. 2010. Timing and duration of garnet granulite metamorphism in magmatic arc crust, Fiordland, New Zealand. Chem Geol, 273: 91–110

Streck M J, Leeman W P, Chesley J. 2007. High-magnesian andesite from Mount Shasta: A product of magma mixing and contamination, not a primitive mantle melt. Geology, 35: 351–354

Su B, Chen Y, Guo S, Chen S, Li Y B. 2019. Garnetite and pyroxenite in the mantle wedge formed by slab-mantle interactions at different melt/rock ratios. J Geophys Res-Solid Earth, 124: 6504–6522

Sun S, McDonough W F. 1989. Chemical and isotopic systematics of oceanic basalts: Implications for mantle composition and processes. Geol Soc Lond Spec Publ, 42: 313–345

Sun W D, Huang R, Li H, Hu Y, Zhang C, Sun S, Zhang L, Ding X, Li C, Zartman R E, Ling M. 2015. Porphyry deposits and oxidized magmas. Ore Geol Rev, 65: 97–131

Sun W D, Liang H, Ling M, Zhan M, Ding X, Zhang H, Yang X, Li Y, Ireland T R, Wei Q, Fan W. 2013. The link between reduced porphyry copper deposits and oxidized magmas. Geochim Cosmochim Acta, 103: 263–275

Tang G J, Wang Q, Wyman D A, Li Z X, Zhao Z H, Jia X H, Jiang Z Q. 2010. Ridge subduction and crustal growth in the Central Asian Orogenic Belt: Evidence from Late Carboniferous adakites and high-Mg diorites in the western Junggar region, northern Xinjiang (west China). Chem Geol, 277: 281–300

Tang G J, Wyman D A, Wang Q, Li J, Li Z X, Zhao Z H, Sun W D. 2012. Asthenosphere-lithosphere interaction triggered by a slab window during ridge subduction: Trace element and Sr-Nd-Hf-Os isotopic evidence from Late Carboniferous tholeiites in the western Junggar area (NW China). Earth Planet Sci Lett, 329-330: 84–96

Tang G J, Wang Q, Wyman D A, Chung S L, Chen H Y, Zhao Z H. 2017. Genesis of pristine adakitic magmas by lower crustal melting: A perspective from amphibole composition. J Geophys Res-Solid Earth, 122: 1934–1948

Tang M, Lee C T A, Costin G, Höfer H E. 2019. Recycling reduced iron at the base of magmatic orogens. Earth Planet Sci Lett, 528: 115827

Tarney J, Jones C E. 1994. Trace element geochemistry of orogenic igneous rocks and crustal growth models. J Geol Soc, 151: 855–868

Tatsumi Y. 2006. High-Mg andesites in the Setouchi Volcanic Belt, southwestern Japan: Analogy to archean magmatism and continental crust formation? Annu Rev Earth Planet Sci, 34: 467–499

Tatsumi Y, Hamilton D L, Nesbitt R W. 1986. Chemical characteristics of fluid phase released from a subducted lithosphere and origin of arc magmas: Evidence from high-pressure experiments and natural rocks. J Volcanol Geotherm Res, 29: 293–309

Tatsumi Y, Ishizaka K. 1981. Existence of andesitic primary magma: An example from southwest Japan. Earth Planet Sci Lett, 53: 124–130

Tatsumi Y, Ishizaka K. 1982a. Origin of high-magnesian andesites in the Setouchi volcanic belt, southwest Japan, I. Petrographical and chemical characteristics. Earth Planet Sci Lett, 60: 293–304

Tatsumi Y, Ishizaka K. 1982b. Magnesian andesite and basalt from Shodo-Shima island, southwest Japan, and their bearing on the genesis of calc-alkaline andesites. Lithos, 15: 161–172

Thiéblemont D, Stein G, Lescuyer J L. 1997. Epithermal and porphyry deposits: The adakite connection. C R Acad Sci Paris, 325: 103–109

Thorkelson D J, Madsen J K, Sluggett C L. 2011. Mantle flow through the Northern Cordilleran slab window revealed by volcanic geochemistry. Geology, 39: 267–270

Thorpe R S, Potts P J, Francis P W. 1976. Rare earth data and petrogenesis of andesite from the North Chilean Andes. Contrib Mineral Petrol, 54: 65–78

Tomascak P B, Ryan J G, Defant M J. 2000. Lithium isotope evidence for light element decoupling in the Panama subarc mantle. Geology, 28: 507–510

Topuz G, Okay A I, Altherr R, Schwarz W H, Siebel W, Zack T, Satır M, Şen C. 2011. Post-collisional adakite-like magmatism in the Ağvanis Massif and implications for the evolution of the Eocene magmatism in the Eastern Pontides (NE Turkey). Lithos, 125: 131–150

Wang C, Song S G, Niu Y L, Su L. 2015. Late Triassic adakitic plutons within the Archean terrane of the North China Craton: Melting of the ancient lower crust at the onset of the lithospheric destruction. Lithos, 212-215: 353–367

Wang C, Song S G, Niu Y L, Allen M B, Su L, Wei C J, Zhang G B, Fu B. 2017. Long-lived melting of ancient lower crust of the North China Craton in response to paleo-Pacific plate subduction, recorded by adakitic rhyolite. Lithos, 292-293: 437–451

Wang L, Kusky T M, Polat A, Wang S J, Jiang X F, Zong K Q, Wang J P, Deng H, Fu J M. 2014. Partial melting of deeply subducted eclogite from the Sulu orogen in China. Nat Commun, 5: 5604

Wang Q, Hawkesworth C J, Wyman D, Chung S L, Wu F Y, Li X H, Li Z X, Gou G N, Zhang X Z, Tang G J, Dan W, Ma L, Dong Y H. 2016. Pliocene-Quaternary crustal melting in central and northern Tibet and insights into crustal flow. Nat Commun, 7: 11888

Wang Q, McDermott F, Xu J F, Bellon H, Zhu Y T. 2005. Cenozoic K-rich adakitic volcanic rocks in the Hohxil area, northern Tibet: Lower-crustal melting in an intracontinental setting. Geology, 33: 465–468

Wang Q, Wyman A, Xu J F, Jian P, Zhao Z H, Li C F, Xu W, Ma J L, He B. 2007a. Early Cretaceous adakitic granites in the Northern Dabie complex, central China: Implications for partial melting and delamination of thickened lower crust. Geochim Cosmochim Acta, 71: 2609–2636

Wang Q, Wyman D A, Xu J F, Dong Y H, Vasconcelos P M, Pearson N, Wan Y S, Dong H, Li C F, Yu Y S, Zhu T X, Feng X T, Zhang Q Y, Zi F, Chu Z Y. 2008. Eocene melting of subducting continental crust and early uplifting of central Tibet: Evidence from central-western Qiangtang high-K calc-alkaline andesites, dacites and rhyolites. Earth Planet Sci Lett, 272: 158–171

Wang Q, Wyman D A, Xu J F, Zhao Z H, Jian P, Xiong X L, Bao Z W, Li C F, Bai Z H. 2006b. Petrogenesis of Cretaceous adakitic and shoshonitic igneous rocks in the Luzong area, Anhui Province (eastern China): Implications for geodynamics and Cu-Au mineralization. Lithos, 89: 424–446

Wang Q, Wyman D A, Xu J F, Zhao Z H, Jian P, Zi F. 2007b. Partial melting of thickened or delaminated lower crust in the middle of eastern China: Implications for Cu-Au mineralization. J Geol, 115: 149–161

Wang Q, Xu J F, Jian P, Bao Z W, Zhao Z H, Li C F, Xiong X L, Ma J L. 2006a. Petrogenesis of adakitic porphyries in an extensional tectonic setting, Dexing, South China: Implications for the genesis of porphyry copper mineralization. J Petrol, 47: 119–144

Wang Q, Xu J F, Zhao Z H, Bao Z W, Xu W, Xiong X L. 2004a. Cretaceous high-potassium intrusive rocks in the Yueshan-Hongzhen area of east China: Adakites in an extensional tectonic regime within a continent. Geochem J, 38: 417–434

Wang Q, Zhao Z H, Bao Z W, Xu J F, Liu W, Li C F, Bai Z H, Xiong X L. 2004b. Geochemistry and petrogenesis of the Tongshankou and Yinzu adakitic intrusive rocks and the associated porphyry copper-molybdenum mineralization in southeast Hubei, east China. Resour Geol, 54: 137–152

Williamson B J, Herrington R J, Morris A. 2016. Porphyry copper enrichment linked to excess aluminium in plagioclase. Nat Geosci, 9: 237–241

Xiao L, Clemens J D. 2007. Origin of potassic (C-type) adakite magmas: Experimental and field constraints. Lithos, 95: 399–414

Xiong X L. 2006. Trace element evidence for growth of early continental crust by melting of rutile-bearing hydrous eclogite. Geology, 34: 945–948

Xiong X L, Adam J, Green T H. 2005. Rutile stability and rutile/melt HFSE partitioning during partial melting of hydrous basalt: Implications for TTG genesis. Chem Geol, 218: 339–359

Xiong X L, Xia B, Xu J F, Niu H C, Xiao W S. 2006. Na depletion in modern adakites via melt/rock reaction within the sub-arc mantle. Chem Geol, 229: 273–292

Xu J F, Shinjo R, Defant M J, Wang Q, Rapp R P. 2002. Origin of Mesozoic adakitic intrusive rocks in the Ningzhen area of east China: Partial melting of delaminated lower continental crust? Geology, 30: 1111–1114

Xu W, Gao S, Wang Q, Wang D, Liu Y. 2006. Mesozoic crustal thickening of the eastern North China Craton: Evidence from eclogite xenoliths and petrologic implications. Geology, 34: 721–724

Xu W L, Gao S, Yang D B, Pei F P, Wang Q H. 2009. Geochemistry of eclogite xenoliths in Mesozoic adakitic rocks from Xuzhou-Suzhou area in central China and their tectonic implications. Lithos, 107: 269–280

Xu W, Hergt J M, Gao S, Pei F, Wang W, Yang D. 2008. Interaction of adakitic melt-peridotite: Implications for the high-Mg$^{\#}$ signature of Mesozoic adakitic rocks in the eastern North China Craton. Earth Planet Sci Lett, 265: 123–137

Xu Y M, Jiang S Y, Zhu Z Y, Yang S Y, Zhou W. 2014. Petrogenesis of Late Mesozoic granitoids and coeval mafic rocks from the Jiurui district in the Middle-Lower Yangtze metallogenic belt of Eastern China: Geochemical and Sr-Nd-Pb-Hf isotopic evidence. Lithos, 190-191: 467–484

Yang Y Z, Chen F, Siebel W, Zhang H, Long Q, He J F, Hou Z H, Zhu X Y. 2014a. Age and composition of Cu-Au related rocks from the lower Yangtze River belt: Constraints on paleo-Pacific slab roll-back beneath eastern China. Lithos, 202-203: 331–346

Yang Y Z, Long Q, Siebel W, Cheng T, Hou Z H, Chen F. 2014b. Paleo-Pacific subduction in the interior of Eastern China: Evidence from adakitic rocks in the Edong-Jiurui District. J Geol, 122: 77–97

Yang Z M, Lu Y J, Hou Z Q, Chang Z S. 2015. High-Mg diorite from Qulong in southern Tibet: Implications for the genesis of adakite-like intrusions and associated porphyry Cu deposits in collisional orogens. J Petrol, 56: 227–254

Yogodzinski G M, Kay R W, Volynets O N, Koloskov A V, Kay S M. 1995. Magnesian andesite in the western Aleutian Komandorsky region: Implications for slab melting and processes in the mantle

wedge. Geol Soc Am Bull, 107: 505–519

Yogodzinski G M, Kelemen P B. 1998. Slab melting in the Aleutians: Implications of an ion probe study of clinopyroxene in primitive adakite and basalt. Earth Planet Sci Lett, 158: 53–65

Yogodzinski G M, Lees J M, Churikova T G, Dorendorf F, Wöerner G, Volynets O N. 2001. Geochemical evidence for the melting of subducting oceanic lithosphere at plate edges. Nature, 409: 500–504

Yogodzinski G M, Volynets O N, Koloskov A V, Seliverstov N I, Matvenkov V V. 1994. Magnesian andesites and the subduction component in a strongly calc-alkaline series at Piip Volcano, Far Western Aleutians. J Petrol, 35: 163–204

Yu H L, Zhang L F, Zhang L J, Wei C J, Li X L, Guo J H, Bader T, Qi Y F. 2019. The metamorphic evolution of Salma-type eclogite in Russia: Constraints from zircon/titanite dating and phase equilibria modeling. Precambrian Res, 326: 363–384

Yu S Y, Li S Z, Zhang J X, Peng Y B, Somerville I, Liu Y J, Wang Z Y, Li Z F, Yao Y, Li Y. 2019. Multistage anatexis during tectonic evolution from oceanic subduction to continental collision: A review of the North Qaidam UHP Belt, NW China. Earth-Sci Rev, 191: 190–211

Yu S Y, Zhang J X, Sun D Y, Li Y S, Gong J H. 2015. Anatexis of ultrahigh-pressure eclogite during exhumation in the north qaidam ultrahigh-pressure terrane: Constraints from petrology, zircon u-pb dating, and geochemistry. Geol Soc Am Bull, 127: 1290–1312

Yumul G P, Dimalanta C, Bellon H, Faustino D V, De Jesus J V, Tamayo R A, Jumawan F T. 2000. Adakitic lavas in the Central Luzon back-arc region, Philippines: Lower crust partial melting products? Island Arc, 9: 499–512

Zellmer G F, Iizuka Y, Miyoshi M, Tamura Y, Tatsumi Y. 2012. Lower crustal H2O controls on the formation of adakitic melts. Geology, 40: 487–490

Zeng L S, Gao L E, Xie K J, Jing L Z. 2011. Mid-Eocene high Sr/Y granites in the northern Himalayan gneiss domes: Melting thickened lower continental crust. Earth Planet Sci Lett, 303: 251–266

Zhang G B, Niu Y L, Song S G, Zhang L F, Tian Z L, Christy A G, Han L. 2015. Trace element behavior and *P-T-t* evolution during partial melting of exhumed eclogite in the North Qaidam UHPM belt (NW China): Implications for adakite genesis. Lithos, 226: 65–80

Zhang L Y, Ducea M N, Ding L, Pullen A, Kapp P, Hoffman D. 2014. Southern Tibetan Oligocene–Miocene adakites: A record of Indian slab tearing. Lithos, 210-211: 209–223

Zhang L, Chen R X, Zheng Y F, Hu Z. 2015. Partial melting of deeply subducted continental crust during exhumation: Insights from felsic veins and host UHP metamorphic rocks in North Qaidam, northern Tibet. J Metamorph Geol, 33: 671–694

Zhao Z F, Liu Z B, Chen Q. 2017. Melting of subducted continental crust: Geochemical evidence from Mesozoic granitoids in the Dabie-Sulu orogenic belt, east-central China. J Asian Earth Sci, 145: 260–277

Zheng Y C, Hou Z Q, Li Q Y, Sun Q Z, Liang W, Fu Q, Li W, Huang K X. 2012. Origin of Late Oligocene adakitic intrusives in the southeastern Lhasa terrane: Evidence from in situ zircon U-Pb dating, Hf-O isotopes, and whole-rock geochemistry. Lithos, 148: 296–311

Zheng Y C, Liu S A, Wu C D, Griffin W L, Li Z Q, Xu B, Yang Z M, Hou Z Q, O'Reilly S Y. 2019. Cu isotopes reveal initial Cu enrichment in sources of giant porphyry deposits in a collisional setting. Geology, 47: 135–138

Zheng Y F. 2019. Subduction zone geochemistry. Geosci Front, 10: 1223–1254

Zheng Y F, Xia Q X, Chen R X, Gao X Y. 2011. Partial melting, fluid supercriticality and element mobility in ultrahigh-pressure metamorphic rocks during continental collision. Earth-Sci Rev, 107: 342–374

Zheng Y F, Hermann J. 2014. Geochemistry of continental subduction-zone fluids. Earth Planet Space, 66: 93

Zheng Y F, Chen Y X. 2016. Continental versus oceanic subduction zones. Natl Sci Rev, 3: 495–519

Zheng Y F, Zhao Z F. 2017. Introduction to the structures and processes of subduction zones. J Asian Earth Sci, 145: 1–15

Zheng Y F, Mao J W, Chen Y J, Sun W D, Ni P, Yang X. 2019. Hydrothermal ore deposits in collisional orogens. Sci Bull, 64: 205–212

Zheng Y F, Chen Y X, Dai L Q, Zhao Z F. 2015. Developing plate tectonics theory from oceanic subduction zones to collisional orogens. Sci China Earth Sci, 58: 1045–1069

Zheng Y F, Xu Z, Chen L, Dai L Q, Zhao Z F. 2020. Chemical geodynamics of mafic magmatism above subduction zones. J Asian Earth Sci, 194: 104185

Zhou J S, Wang Q, Wyman D A, Zhao Z H. 2020a. Petrologic reconstruction of the Tieshan magma plumbing system: Implications for the genesis of magmatic-hydrothermal ore deposits within originally water-poor magmatic systems. J Petrol, doi: 10.1093/petrology/egaa056

Zhou J S, Yang Z S, Hou Z Q, Wang Q. 2020b. Amphibole-rich cumulate xenoliths in the Zhazhalong intrusive suite, Gangdese arc: Implications for the role of amphibole fractionation during magma evolution. Am Miner, 105: 262–275

(责任编委: 郑永飞)